

Metal–Organic Frameworks as Platforms for Catalytic Applications

Long Jiao, Yang Wang, Hai-Long Jiang,* and Qiang Xu*

Dedicated to Prof. Susumu Kitagawa on the occasion of his 65th birthday

Metal–organic frameworks (MOFs), also called porous coordination polymers, represent a class of crystalline porous materials built from organic linkers and metal ions/clusters. The unique features of MOFs, including structural diversity and tailorability as well as high surface area, etc., enable them to be a highly versatile platform for potential applications in many fields. Herein, an overview of recent developments achieved in MOF catalysis, including heterogeneous catalysis, photocatalysis, and electrocatalysis over MOFs and MOF-based materials, is provided. The active sites involved in the catalysts are particularly emphasized. The challenges, future trends, and prospects associated with MOFs and their related materials for catalysis are also discussed.

1. Introduction

Emerging as a relatively new class of porous solid materials, metal–organic frameworks (MOFs), also called porous coordination polymers (PCPs), being constructed by metal ions/clusters and organic linkers, have captured widespread interest and achieved the explosive development over the past two decades.^[1,2] The crystalline nature, structural diversity, and tailorability as well as ultrahigh surface area make MOFs find their potential applications in diverse fields, such as gas sorption and separation, chemical sensing, proton conductivity, biomedicine, etc.^[1–8] In particular, catalysis is one of the earliest demonstrated applications^[9]

and becoming one of the most promising applications for MOFs, along with its rapid development in the past 20 years.^[10–13]

In view of structure, MOFs are similar to homogeneous catalysts, typically, transition metal complex, which is alternatively regarded as an isolated unit in the infinite network of MOFs. Moreover, the periodic structure enables MOFs to disperse active sites uniformly throughout the framework; the porosity facilitates the accessibility of active sites and the transport of catalytic substrates/products in MOFs. Therefore, MOFs might behave like metal complex catalysts and possess the advantages

of homogeneous catalysis. On the other hand, being porous solid materials, MOFs are well recyclable after catalytic runs—a character endowed by heterogeneous catalysts. Therefore, MOFs are the particular catalysts that are able to integrate the respective merits between “homogeneous catalyst (e.g., metal complex)—full usage of active sites and high reactivity” and “heterogeneous catalyst—recyclability.”


In comparison with the traditional porous catalysts, such as zeolite, activated carbon, etc., MOFs have much more diversified structures featuring highly tunable pore sizes (usually 0–3 nm, up to 9.8 nm), which are deemed to bridge the pore size gap between microporous zeolites and mesoporous materials. The uniform pore size/shape allows the accessibility of reaction substrates or products with specific shape/size, endowing the selective catalysis of MOFs. Moreover, their very high surface area (BET, usually >1000 m² g⁻¹, up to 7000 m² g⁻¹) favors the adsorption and enrichment of substrate molecules around the active sites, further benefiting the subsequent activation and catalytic conversion. Particularly, the crystalline nature endows MOFs with well-defined structures, which are of vital importance to understand the underlying mechanism and relationship between structure and catalytic performance. In addition, some pore structure design approaches, such as pore space partition, are also important for catalytic properties of MOFs.^[14,15] The smaller pores after pore partition in MOFs might improve host–guest interactions and thus merit catalytic efficiency. Particularly, the pore-partition strategy can be employed to insert unusual heterometallic species into MOFs, which would be also beneficial to the catalytic properties.^[14,16] Therefore, MOFs, being special solid catalysts, are very promising, especially in fundamental catalysis.

The catalytic centers involved in pristine MOFs are usually limited to the coordinatively unsaturated metal sites (CUSs)-Lewis acid centers and/or the active group on the organic

L. Jiao, Dr. Y. Wang, Prof. H.-L. Jiang
Hefei National Laboratory for Physical Sciences at the Microscale
CAS Key Laboratory of Soft Matter Chemistry
Collaborative Innovation Center of Suzhou Nano Science and
Technology
Department of Chemistry
University of Science and Technology of China
Hefei, Anhui 230026, P. R. China
E-mail: jianglab@ustc.edu.cn

Prof. Q. Xu
Research Institute of Electrochemical Energy
National Institute of Advanced Industrial Science and Technology (AIST)
1-8-31 Midorigaoka, Ikeda, Osaka 563-8577, Japan
E-mail: q.xu@aist.go.jp

Prof. Q. Xu
AIST-Kyoto University Chemical Energy Materials Open Innovation
Laboratory (ChEM-OIL)
Yoshida, Sakyo-ku, Kyoto 606-8501, Japan

 The ORCID identification number(s) for the author(s) of this article can be found under <https://doi.org/10.1002/adma.201703663>.

DOI: 10.1002/adma.201703663

linkers (usually acid/base sites). This situation actually limits MOFs to a certain scope of catalytic reactions. Fortunately, the predicament can be well addressed based on at least two approaches: (a) functionalized modification—it is possible to graft desired active sites onto either metal ions/clusters or organic linkers by the multivariate approach^[17] or postsynthetic modification;^[18] (b) pore confinement/encapsulation. The pore space of MOFs is able to accommodate a variety of additional active species (e.g., organic molecules, and inorganic nanoparticles, metal complexes, enzymes) as guests and behave as nano-reactor to host catalytic reactions (Figure 1).

Apart from the heterogeneous organic reactions over MOFs or MOF-based composites by aforementioned modification or inclusion, facing the global energy crisis and environmental issues, MOFs and MOF-based materials have also been demonstrated to be promising in photocatalysis and electrocatalysis for clean energy. Many MOFs possessing semiconductor-like behavior have primarily shown their advantages in photocatalysis, typically in water splitting and CO₂ reduction.^[19,20] The high porosity of MOFs would greatly suppress the classical volume recombination of electron–hole, thanks to the short transport distance of charge carriers to the pore surface throughout the structure for reactions; the great crystallinity also avoids the defects that might produce recombination centers. The introduction of additional electron acceptors can further improve the charge separation and photocatalytic efficiency. In addition, given the extreme conditions required in some catalytic systems, especially in electrocatalysis (strong acidic/alkaline solutions), most of the MOFs are prone to be disassembled and only a few of them are applicable directly as electrocatalysts. In this case, the conversion of MOFs as precursors/templates, together with additives if necessary, to diverse nanocomposites with pore character partially inherited from their parent MOFs has been extensively explored.^[21,22] The obtained materials with large surface area and highly dispersed active sites were found to be important in both heterogeneous catalysis and electrocatalysis.^[23–27] In this review, we summarize recent progress of MOFs for heterogeneous catalysis by the categorization with catalytic reactive sites and then highlight the recent development of MOF-based catalysts for photocatalysis and electrocatalysis. Particular challenges of MOFs and their related materials as well as research opportunities for further development toward catalysis are critically discussed.

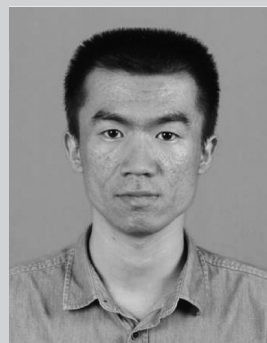
2. MOFs for Heterogeneous Catalysis

2.1. Pristine Framework Activity

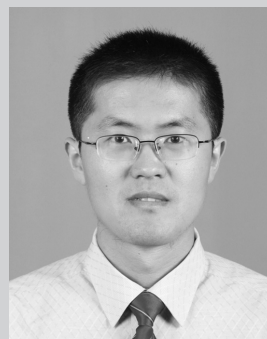
2.1.1. Active Sites at Metal Nodes

The metal ions in MOFs are coordinated by organic ligands and possibly solvent molecules, the latter of which can be readily removed by heating or evacuation with retained framework structures, leaving the CUSs in metal nodes. The CUSs can act as typical Lewis acid centers for accepting electrons from the substrates and promoting their conversion to products.

The classical HKUST-1 gives open Cu²⁺ sites upon the removal of coordinated water molecules by heating, exhibiting sound Lewis acid activity in the cyanosilylation of benzaldehyde



Long Jiao received his B.S. degree in materials physics from Shandong University in 2014. He is currently a Ph.D. student under the guidance of Prof. Hai-Long Jiang at the University of Science and Technology of China (USTC). His research work is focused on the development of metal–organic-framework-based materials for electrocatalysis.



Hai-Long Jiang received his Ph.D. in 2008 from Fujian Institute of Research on the Structure of Matter, Chinese Academy of Sciences and then worked at AIST (Japan) as a postdoc and JSPS fellow in 2008–2011. After a post-doctoral stint at Texas A&M University (USA), he accepted a full professorship to start his independent career at

University of Science and Technology of China in 2013. His main research interest is in the development of crystalline porous and nanostructured materials, crossing coordination chemistry and nanoscience, for energy-/environment-related catalysis.



Qiang Xu received his Ph.D. in physical chemistry in 1994 from Osaka University. He is the Director of the AIST-Kyoto University Chemical Energy Materials Open Innovation Laboratory (ChEM-OIL), an Adjunct Professor at Kobe University and at Kyoto University, a Specially Appointed Distinguished Professor at Yangzhou

University, and a Distinguished Honorary Professor at the Hong Kong Polytechnic University. His research interests include the chemistry of nanostructured materials and their applications, especially for energy.

and the isomerization of terpene derivatives.^[28,29] Another classical MIL-101(Cr), composed of trimeric chromium(III) octahedral clusters interconnected by 1,4-benzene-dicarboxylate (BDC) anions, exerts Lewis acidity upon the removal of the terminally coordinated H₂O molecules for better activity than HKUST-1 in the cyanosilylation of aldehydes due to the greater Lewis acidity of Cr(III) than Cu(II).^[30] Long and co-workers reported a 3D porous Mn₃[(Mn₄Cl)₃BTT₈(CH₃OH)₁₀]₂ (H₃BTT = 1,3,5-benzenetris(tetrazol-5-yl)), built from chloride-centered

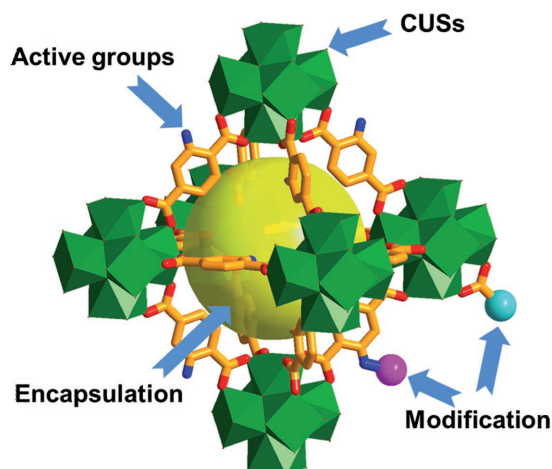


Figure 1. Different strategies to the incorporation of active species inside a MOF.

square-planar $[\text{Mn}_4\text{Cl}]^{7+}$ units linked by BTT^{3-} ligands with 7 and 10 Å pores, for cyanosilylation of benzaldehyde (Figure 2a).^[31] The MOF catalyst exhibited high conversion and good size selectivity for the substrates due to the pore size exclusion effect, and IR spectra confirmed the activation of reactants on the exposed Mn(II) centers.

The NU-1000, with Lewis-acidic Zr(IV) ions as active sites and 1D mesoporous channels, have been reported for acid-catalyzed hydrolysis of phosphate ester reactions, showing faster efficiency than other MOF-based catalysts.^[32] Right after,

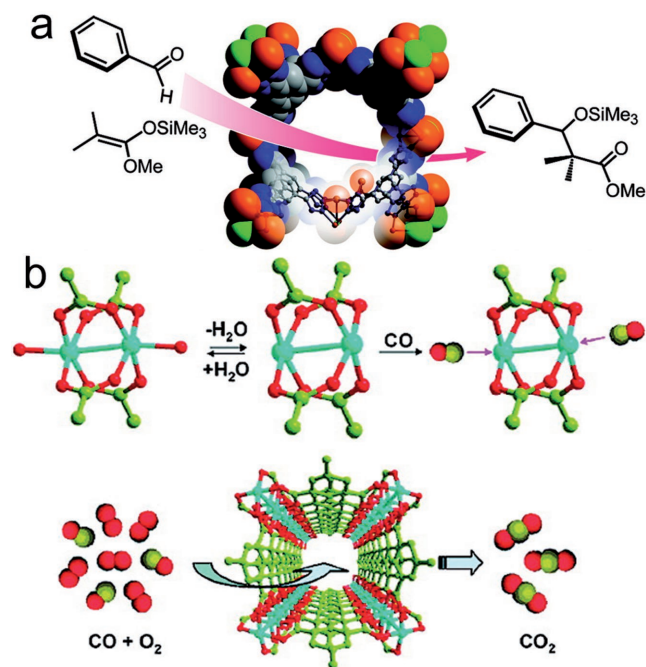


Figure 2. a) The benzaldehyde cyanosilylation reaction over $\text{Mn}_3[(\text{Mn}_4\text{Cl})_3\text{BTT}_8(\text{CH}_3\text{OH})_{10}]_2$. Adapted with permission.^[31] Copyright 2008, American Chemical Society. b) Schematic diagram showing the oxidation of CO to CO_2 by dehydrated $[\text{Cu}(\text{mipt})(\text{H}_2\text{O})_2](\text{H}_2\text{O})_2$. Reproduced with permission.^[34] Copyright 2007, American Chemical Society.

the same group chose MOF-808, featuring 6-connected Zr-oxo nodes, to catalyze the hydrolysis of phosphate ester, exhibiting higher hydrolysis rates than UiO-66 (12-connected Zr-oxo nodes) and even NU-1000 (8-connected Zr-oxo nodes).^[33] In addition to liquid-phase catalysis, MOFs featuring Lewis acidity are also applicable to gas-phase reactions. Xu and co-workers presented a MOF of Cu(mipt) (mipt = 5-methylisophthalate) involving open Cu(II) sites, which were evidenced by using ^{12}C O and ^{13}C O probe molecules, for excellent and stable catalysis toward the CO oxidation to CO_2 (Figure 2b).^[34]

Engineering structural defects in MOFs leads to extra exposed metal centers that are active in catalysis.^[35] De Vos and co-workers used trifluoroacetic acid (TFA) as a modulator to synthesize UiO-66 with different levels of defects.^[36] Without affecting the crystallization of UiO-66, TFA replaced a part of terephthalate linkers and created extra Lewis acid sites, resulting in enhanced activity for the Meerwein reduction of 4-*tert*-butylcyclohexanone (TCH) in reference to the parent MOF. Jiang and co-workers synthesized a stable Al-based MOF based on 4,4'-dibenzoic acid-2,2'-sulfone linker, denoted as USTC-253.^[37] TFA was added as the modulator during the synthesis of USTC-253, causing the competitive coordination with organic ligands. Upon removing TFA, the additional unsaturated Al centers and polar $-\text{SO}_2$ group in USTC-253-TFA led to higher CO_2 uptake and better activity than USTC-253 toward CO_2 cycloaddition with epoxides.

In reference to Lewis acidity, Brønsted acidity in MOFs is usually stronger and shows much higher activity for acid-catalyzed reactions. Férey and co-workers reported the catalytic activity of MIL-100(Fe) for Friedel–Crafts benzylation.^[38] The MIL-53(Ga) $[\text{Ga}(\mu_2\text{-OH})(\text{BDC})]$, with rod-shaped structure containing bridging hydroxyl groups serving as Brønsted acid sites, exhibited high activity toward Friedel–Craft alkylation of aromatic.^[39] An Hf-based MOF (Hf-NU-1000) with strong Hf–O bonds, when serving as a Brønsted acid catalyst demonstrated high catalytic efficiency for the cycloaddition reactions of CO_2 with epoxides.^[40]

2.1.2. Active Sites at Organic Linkers

Functional groups on organic linkers can be tailored for heterogeneous catalysis. There are a variety of functional groups serving as active sites for catalysis, such as amino, amide, pyridyl, sulfoxy, bipyridyl, etc. The active functional groups can be linked to the MOF ligands, thereby resulting in a stable catalytic system.

The sulfonic acid group ($-\text{SO}_3\text{H}$) was grafted onto the aromatic linker to fabricate MOFs, such as MIL-101(Cr). Kitagawa and co-workers prepared partially protonated $-\text{SO}_3\text{Na}$ group functionalized MIL-101(Cr) by using 2-sulfoterephthalate in the presence of HCl.^[41] With the strong Brønsted acid site on its pore surface, this MOF showed high activity in the catalytic cellulose hydrolysis. Recently, Jiang and co-workers reported an $\approx 100\%$ sulfonic acid functionalized MOF, MIL-101- SO_3H , by a postsynthetic HCl treatment strategy, showing excellent catalytic performance in the ring opening of styrene oxide in methanol.^[42] Carboxylic acid as Brønsted acid was also incorporated into the organic linkers in MOFs to catalyze the ring-opening methanolysis of a small, cavity-accessible epoxide.^[43]

It is possible to obtain MOF basic catalysts by incorporating basic functional groups like pyridyl, amide, and amino

in organic linkers.^[44] These MOF basic catalysts have been employed in the Knoevenagel condensation and transesterification reactions. Kim and co-workers synthesized a homochiral MOFs, α -POST-1 with 1D channels by using the pyridyl group functionalized organic linker.^[45] The framework structure showed that a half of pyridine groups extrude into the channel, providing the basic sites for the transesterification of 2,4-dinitrophenyl acetate. Kitagawa and co-workers reported a 3D coordination network based on a tridentate amide ligand containing three pyridyl groups as coordination sites and three amide groups as guest interaction sites.^[46] The highly ordered amide groups on the walls of the channels offer base sites for Knoevenagel condensation reactions of benzaldehyde. Similarly, amino-functionalized MOFs confirmed that the amino group was also capable of performing base-catalyzed Knoevenagel condensation of benzaldehyde with ethyl cyanoacetate and ethyl acetoacetate.^[47]

MOFs are unique heterogeneous catalytic system as different types of catalytic sites, for example, acid and base sites, can be precisely installed within one MOF without mutual interference. Gao and co-workers reported a new MIL-101 dually functionalized with amino and sulfo groups for one-pot deacetalization-Knoevenagel condensation.^[48] De Vos and co-workers obtained an amino-functionalized MOF, UiO-66-NH₂, containing Lewis-acidic Zr⁴⁺ sites and basic amino groups, as a bifunctional acid–base catalyst for one-pot tandem reaction between heptanal and benzaldehyde.^[49]

In addition to the acidic and basic catalysis over MOFs, the heterogenization of molecular catalysts (porphyrins, salens, etc.) by employing them as building units to fabricate MOFs is very attractive. Hupp and co-workers developed a series of Zn-metalloporphyrinic MOFs with different metal residing inside the porphyrin center and these MOFs were found to be effective catalysts for both epoxidation and hydroxylation reactions.^[50,51] Based on facile solvothermal reactions of metalloporphyrinic ligands and M(NO₃)₂ (M = Zn, Cd), Wu and co-workers also reported a series of metalloporphyrinic MOFs, which displayed recyclable activity in the epoxidation of olefins, much better than the corresponding homogeneous metalloporphyrinic complexes.^[52,53]

Many porphyrinic MOFs cannot remain stable toward water environment until the development of Zr-porphyrin MOF, PCN-222 (also called MOF-545, MMPF-6),^[54–56] which is constructed by Zr₆ cluster and M-TCPP (H₂TCPP = tetrakis(4-carboxyphenyl)-porphyrin), possessing large 1D open channels with a diameter of up to 3.7 nm (Figure 3a). The PCN-222(Fe) was used for mimicking cytochrome P450 enzymes and exhibited excellent peroxidase-like catalytic activity owing to its exceptional stability, mesoporosity, and high density of metalloporphyrin centers. Subsequently, Zhou and co-workers developed a series of highly stable Zr-porphyrinic MOFs, including PCN-224(M) M = 2H, Ni, Co, Fe), which feature a 3D network channels with 1.9 nm of pores and high stability in a wide pH range from 0 to 11. The PCN-224(Co) was employed as a reusable heterogeneous catalyst for the CO₂ and epoxide cycloaddition reactions.^[57]

Salens, a class of universal chelate ligands, can accommodate various metal ions for efficient catalysis. Moreover, motivated by excellent asymmetric catalytic activities of homogeneous metallosalen complexes, MOFs involving chiral metallosalen building blocks have attracted great interest and

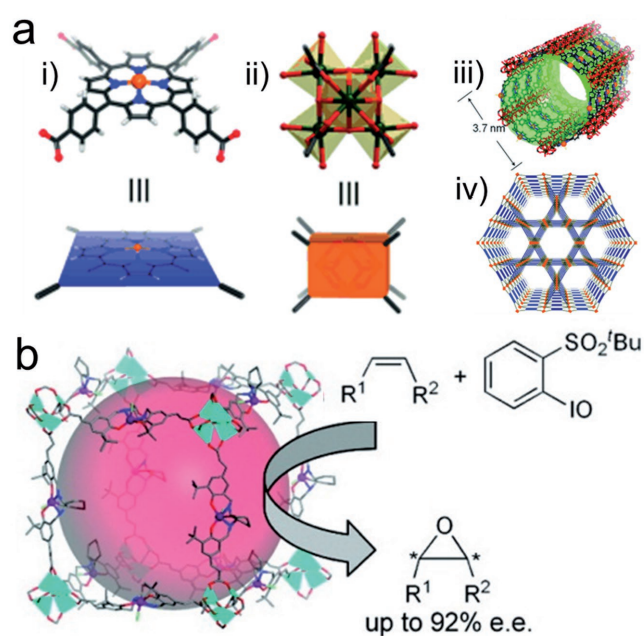


Figure 3. a) Crystal structure and underlying network topology of PCN-222(Fe). The Fe-TCPP (i; blue square) is connected to four 8-connected Zr₆ clusters (ii; light orange cuboid). Adapted with permission.^[54] Copyright 2012, Wiley-VCH. b) Isoreticular chiral MOF assembled from Zn₄(μ₄-O)(O₂CR)₆ SBUs and Mn-salen-derived dicarboxylic acids for asymmetric alkene epoxidation. Adapted with permission.^[60] Copyright 2010, American Chemical Society.

showed effective asymmetric catalytic activity with high enantioselectivity. Two zinc paddlewheel MOFs, the catenated Zn₂(bpdC)₂(Mn-salen) and noncatenated Zn₂(tcpb)(Mn-salen), with accessible Mn^{III} sites in the channels showed outstanding activity toward asymmetric epoxidation reactions with high size selectivity for substrates.^[58,59] A series of iso-reticular chiral MOFs (CMOFs), which were assembled from Zn₄(μ₄-O)(O₂CR)₆ secondary building units (SBUs) and Mn-salen-derived dicarboxylic acids, featuring tunable open channel sizes were successfully employed by Lin and co-workers for asymmetric epoxidation reactions (Figure 3b).^[60,61] More recently, Cui and co-workers synthesized a MOF based on Cd(NO₃)₂·6H₂O and Co(salen-2)(OAc) to afford Co(salen)-based MOF with a 3D chiral nanoporous framework, which showed efficient and recyclable heterogeneous activity for hydrolytic kinetic resolution of racemic epoxides.^[62]

Lin and co-workers designed a 3D homochiral porous MOF from Cd(II) and a BINOL (BINOL = 1,1'-bi-2-naphthol) type chiral bridging ligand that contains pyridyl and orthogonal dihydroxy functionalities.^[63] The catalytic experiments revealed that the Ti(OⁱPr)₄-treated MOF catalyzed the addition of ZnEt₂ to 1-naphthaldehyde with complete conversion of (R)-1-(1-naphthyl)propanol and 93% enantiomeric excess (ee). Further studies showed that the modified homochiral MOF also catalyzed the addition of ZnEt₂ to a range of aromatic aldehydes with complete conversion and ee values similar to the related homogeneous catalyst. Cui and co-workers reported a homochiral MOF constructed by enantiopure 2,2'-dihydroxy-1,1'-iphenyl ligands.^[64] After exchanging one proton of the dihydroxyl group with Li(I) ions, the MOF became highly efficient

for asymmetric cyanation of aldehydes with up to >99% ee. Compared with the homogeneous counterpart, the MOF catalyst also exhibited significantly enhanced activity and enantioselectivity, especially at a low catalyst/substrate ratio.

2.2. Functionalized Modification

The synthetically chemical modifications are an effective and powerful way to introduce certain functionalities into MOF materials for specialized and sophisticated applications, which usually cannot be realized through traditional synthetic methods. The ability to modify the physical environment of the pores and cavities within MOFs would regulate the interaction with substrates and thus reactivity. MOFs can be functionally modified via their metal nodes and organic linkers, as well as the incorporation of guest species into pore space, through various synthetic approaches.

2.2.1. Functionalized Modification for Metal Nodes

The CUSs of MOFs allow the modification with active species through chemical binding. Férey and co-workers revealed that dehydrated MIL-101(Cr) provided CUSs for the coordination of different amine groups, serving as the base catalyst toward Knoevenagel condensation reactions.^[65]

Banerjee et al. reported the synthesis of chiral MIL-101 by postsynthetic modification with catalytically active chiral molecules (Figure 4a).^[66] They chose L-proline as a chiral catalytic unit to bind with the unsaturated metal sites that transformed

MIL-101 into chiral MOF with retained XRD pattern and N₂ adsorption isotherms. The catalytic activities of chiral MIL-101 were evaluated in asymmetric aldol reactions between various aromatic aldehydes and ketones, presenting 60–90% yields with 55–80% enantioselectivity that is much better than unmodified MIL-101 (0% enantioselectivity) and the homogeneous chiral molecule (29% enantioselectivity), and the resultant chiral MOF can be reused up to three times without much change in yield and enantioselectivity.

Except for the modification of CUSs with organic molecules, on the basis of the grafting of metal complex onto M-oxo nodes, MOFs have also been developed as the potential platform for heterogeneous single-site catalysis very recently.^[67–71] Yang et al. introduced Iridium complexes to metal nodes of UiO-66 and NU-1000 for the catalysis of ethylene hydrogenation.^[67] Similarly, Noh et al. explored the deposition of a catalytically active molybdenum(VI) oxide onto the Zr₆ nodes of NU-1000 via solvothermal deposition strategy.^[68] The obtained Mo-SIM catalyst exhibited an exceptional conversion of 93 ± 2% for cyclohexene epoxidation after 7 h reaction at 60 °C under N₂. The atomic layer deposition (ALD) technique, as one of the powerful approaches to anchor single sites to metal nodes of different MOFs, was also exploited by Farha and Hupp's group. For instance, by installing Ni ions precisely on the Zr-oxo nodes in NU-1000 through ALD technology, Li et al. obtained single nickel sites (denoted as Ni-AIM) and used them for gas-phase hydrogenation of ethylene, showing a long-term stability.^[69] Lin and co-workers also make great contribution to the development of single-site catalysis of MOFs. They prepared UiO-68(Zr) and used Zr-oxo clusters to anchor a single-site catalyst (Figure 4b).^[70] They chose *n*BuLi to deprotonate the

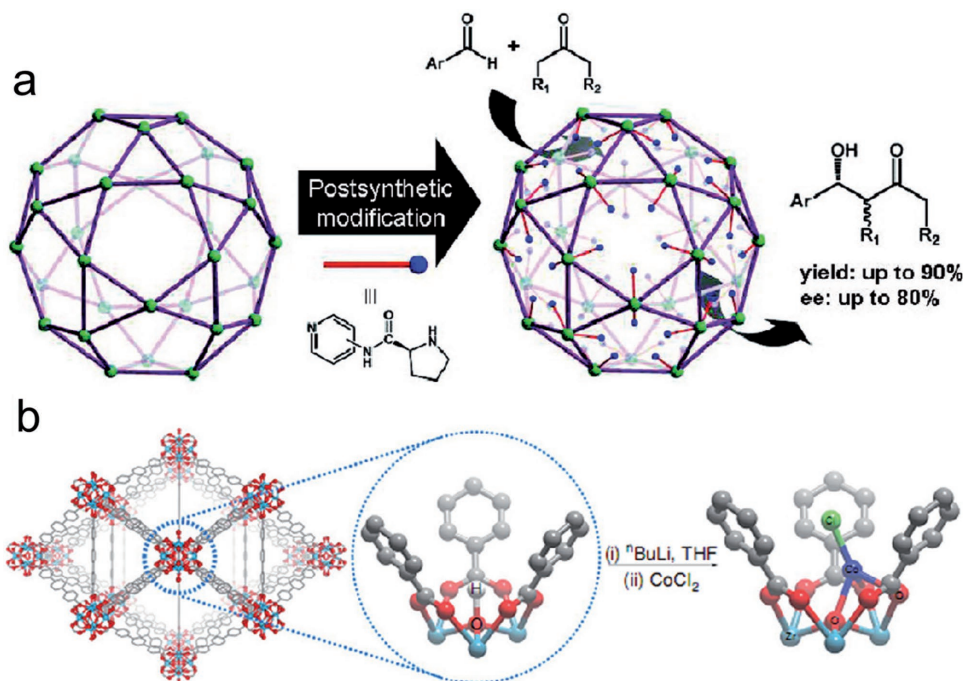


Figure 4. a,b) Schematic illustrations showing the synthesis of chiral MIL-101 by postsynthetic modification with chiral molecules for chiral catalysis (a) and the postsynthetic metalation of the SBUs of UiO-68 with CoCl₂ (b). a) Reproduced with permission.^[66] Copyright 2009, American Chemical Society. b) Reproduced with permission.^[70] Copyright 2016, Nature Publishing Group.

–OH groups, followed by reaction with CoCl_2 or $\text{FeBr}_2 \cdot 2\text{THF}$ to afford the Co- or Fe-functionalized UiO-68. The obtained catalysts showed excellent catalytic activity for benzylic C–H silylation and benzylic C–H borylation. Using a similar methodology, they also created a single-site catalyst by metalation of the MOF, $\text{M}'\text{-MTBC}$ ($\text{M}' = \text{Zr}$ or Hf , MTBC = methanetetrakis(*p*-biphenylcarboxylate), with CoCl_2 , followed by treatment with NaBEt_3H , afforded highly active and reusable solid Zr-MTBC-CoH catalysts for the hydrogenation of alkenes, imines, carbonyls, and heterocycles.^[71]

2.2.2. Functionalized Modification for Organic Linkers

The functional species (e.g., organic molecules, metal complex, and chiral molecules) can also be introduced into organic linkers of MOFs by functionalized modification approach. Bloch et al. prepared MOF-253 [$\text{Al}(\text{OH})(\text{bpydc}); \text{bpydc} = 2,2'$ -bipyridine-5,5'-dicarboxylate], where the 2,2'-bipyridine (bpy) moieties provide a platform for the insertion of various metal centers, such as PdCl_2 (Figure 5a).^[72] Considering that uncoordinated bidentate chelating centers, Carson et al. further used MOF-253 for the immobilization of a ruthenium complex to give MOF-253-Ru, which showed efficient oxidation of alcohols to aldehydes.^[73] The new hybrid catalysts IRMOF-3Lr and UiO-66-NH₂Lr ($\text{Ir} = \text{iridium}$; $\text{L} = 6$ -((diisopropyl-amino)methyl)picolinaldehyde) were synthesized by introducing the activity of Ir complex into IRMOF-3 and UiO-66-NH₂ for the synthesis of *N*-alkyl amines via reductive amination of aldehydes with nitroarenes in the presence of hydrogen (Figure 5b).^[74] The obtained IRMOF-3Lr and UiO-66-NH₂Lr with good thermal stability were used to create a variety of *N*-alkyl amines in good

to excellent yields. A molecular nickel complex was anchored to a mesoporous MOF (Ni@Fe-MIL-101) via postfunctionalization, generating a very active and reusable catalyst for the liquid-phase ethylene dimerization to selectively give 1-butene (Figure 5c).^[75] The Ni@Fe-MIL-101 catalyst presented higher selectivity to 1-butene than those of molecular nickel diimino complexes.

2.3. Encapsulation of Guest Species in MOFs

Despite the advantages of MOFs for catalysis indicated above, the type of active sites on pristine MOFs is mainly limited to the following two sources, unsaturated metal centers and organic ligands, resulting in the reactivity toward limited reactions. In addition to the above two approaches introducing active sites, as porous materials, MOFs are able to accommodate guest species (e.g., metal complexes, enzyme, and metal NPs (MNPs)) into their pore space by a noncovalent interaction, and the resulting guest@MOFs can serve as a multifunctional platform for their synergistic effect in catalytic reactions, largely extending the application of MOFs in catalysis.

2.3.1. Metal Complexes/Macromolecules

Eddaoudi and co-workers chose 4,5-imidazole dicarboxylic acid as the organic linker connecting with $\text{In}(\text{NO}_3)_3$ to create an anionic zeolite-like MOF (denoted as rho-ZMOF) with large cavities, which can provide enough space to encapsulate cationic porphyrins via electrostatic interaction during synthetic process, and the relatively small pore opening can prevent

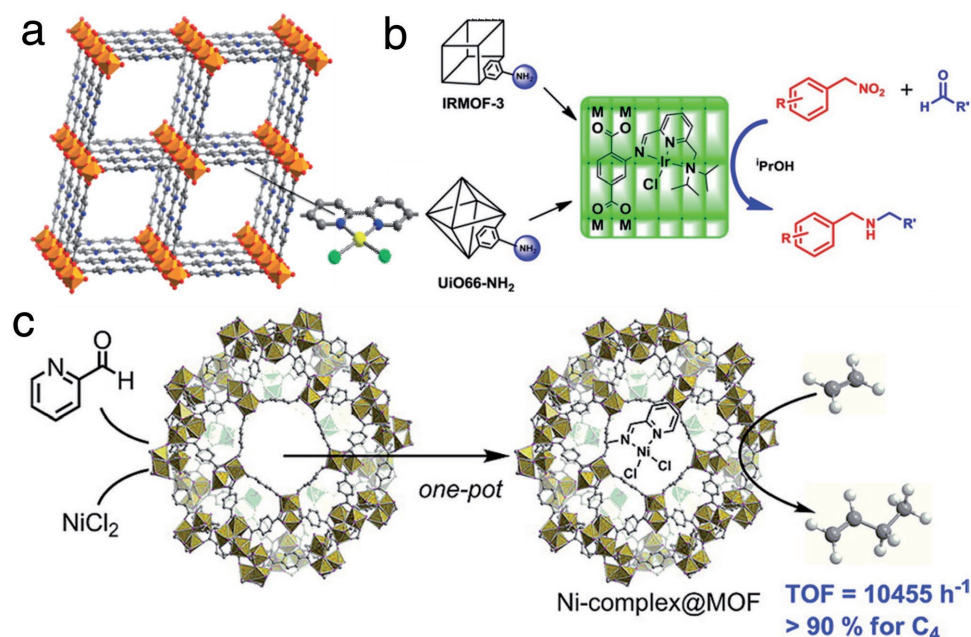


Figure 5. a) The structure of $\text{Al}(\text{OH})(\text{bpydc})$ (MOF-253) with subsequent insertion of PdCl_2 into open bpy ligand. Adapted with permission.^[72] Copyright 2010, American Chemical Society. b) Schematic representation of postmodification of IRMOF-3 and UiO-66-NH₂ with Ir complex for one-pot cascade reaction. Adapted with permission.^[74] Copyright 2013, Elsevier. c) Schematic illustration of the synthesis of Ni(II) complex@Fe-MIL-101 for selective ethylene dimerization. Reproduced with permission.^[75] Copyright 2013, American Chemical Society.

porphyrins from crossing freely with confinement effect.^[76] The resultant Mn-porphyrin encapsulated rho-ZMOF showed a high yield for the oxidation of cyclohexane to cyclohexanol and cyclohexanone. Using a similar synthetic strategy, metalloporphyrin was immobilized into HKUST-1 for mimicking heme enzymes in terms of both structure and reactivity.^[77]

Farrusseng and co-workers used the wet infiltration method to encapsulate metal phthalocyanine complexes in cavities of Cr-MIL-101 for selective oxidation of tetralin into 1-tetralone.^[78] Unfortunately, the coassembly approach or wet infiltration method usually induces some guest molecules to be adsorbed on the MOF surface. In view of this situation, Ma and co-workers developed a metal-action-directed de novo assembly strategy to encapsulate the functionalized guest molecules into a MOF (Figure 6a).^[79] With an anionic bio-MOF-1, positively charged Co^{2+} ions were first exchanged into its framework by electrostatic interaction, which was then reacted with 1,2-dicyanobenzene to form cobalt(II) phthalocyanine (Co-Pc) assembled in bio-MOF-1 nanopores via confinement effect. The resultant Co-Pc@bio-MOF-1 showed a relatively high activity to catalyze styrene epoxidation reaction, whose activity was superior to the homogeneous Co-Pc counterpart.

2.3.2. Polyoxometalates (POMs)

POMs play an important role in various fields including acid and oxidation catalysis. Unfortunately, they always suffer from small surface areas ($<10 \text{ m}^2 \text{ g}^{-1}$), low stability under

catalytic conditions, and high solubility in aqueous solution, severely limiting their applications.^[80,81] Immobilization of POMs into MOFs is a promising approach to stabilize POMs and optimize their catalytic performance. Liu, Su and co-workers reported a simple one-pot hydrothermal route to incorporate $\text{H}_n\text{XM}_{12}\text{O}_{40}$ ($\text{X} = \text{Si, Ge, P, As; M} = \text{W, Mo}$) into the porous MOF to give POM@HKUST-1 composites (Figure 6b).^[82,83] Given the encapsulation of the strong Brønsted acid of $\text{H}_3\text{PW}_{12}\text{O}_{40}$ (HPW) species, the HPW@HKUST-1 composites showed extremely high catalytic activity and good stability for ethyl acetate hydrolysis, far superior to most of the inorganic solid acids. It was worthy emphasizing that HPW@HKUST-1 also displayed great potential in the elimination of nerve gas. With good adsorption capability for the nerve gas simulant of dimethyl methylphosphonate (DMMP), the HPW@HKUST-1 composites can decompose DMMP through a simple hydrolysis reaction. The conversion of DMMP to methyl alcohol was 34% at room temperature and increased gradually with elevated temperature, reaching 93% at $50 \text{ }^\circ\text{C}$.^[82] The similar phenomenon was also observed in the esterification reaction of acetic acid with 1-propanol catalyzed by HPW@HKUST-1.^[84]

Not limited to the incorporation of pure HPW into MOFs, Hill and co-workers further explored POM@HKUST-1 by incorporating Cu containing Keggin-type polyoxometalate units [$\text{CuPW}_{11}\text{O}_{39}$].^[85] It was observed that the stability of both components was mutually enhanced due to the synergistic effect between POM and MOF. The interactions also dramatically improved catalytic activity of the POM for air-based oxidative decontamination of various toxic sulfur compounds including H_2S to S_8 . In addition, size- and shape-dependent selectivity was clearly observed in the oxidation of the evaluated mercaptans to disulfides. In addition, small pore sizes of most MOFs (usually in a microporous size regime) always restrict the loading of active large molecules, such as POMs. Facing to these challenges, Cai and Jiang developed a versatile modulator-induced defect-formation strategy to realize the controllable synthesis of hierarchically porous MOFs (HP-MOFs) with high stability for encapsulating large active POMs.^[86] With a higher loading content of active HPW into the HP-UiO-66, the resultant $\text{H}_3\text{PW}_{12}\text{O}_{40}$ -impregnated HP-UiO-66 (HPW/HP-UiO-66) gave significantly higher activity and stability than HPW-impregnated UiO-66 (HPW/UiO-66).

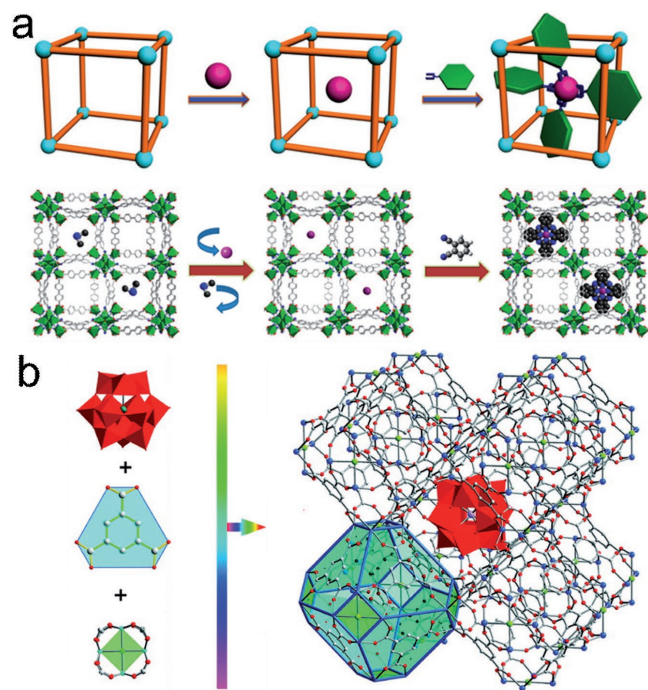


Figure 6. a) The de novo assembly of Co-Pc@bio-MOF-1. Reproduced with permission.^[79] Copyright 2014, American Chemical Society. b) Templated self-assembly of POM@HKUST-1 composites by simply mixing MOF precursors and polyanions. Adapted with permission.^[82] Copyright 2011, American Chemical Society.

2.3.3. Metal Nanoparticles

The crystalline porous structure of MOFs offers inherent conditions to stabilize small MNPs, preventing them from the common aggregation and thus benefiting to the activity and stability of catalysts.^[87] There are two main approaches to the immobilization of MNPs in MOFs. The first approach is known as “ship-in-a-bottle” route: the metal precursors are immersed into presynthesized MOF pores through solution infiltration, vapor deposition, or solid grinding strategy, and then are reduced to MNPs through various reducing agent, such as hydrogen, ammonia borane, NaBH_4 , etc. The ship-in-a-bottle strategy has been demonstrated to be an efficient way to generate ultrafine MNPs in MOFs.

Fischer and co-workers used a chemical vapor deposition (CVD) technique to introduce gas-phase organometallics as the metal precursors.^[88–90] In a typical synthesis, the chosen MOF is exposed to the vapor of gas-phase organometallic precursors under static vacuum. The volatile precursors diffuse into the MOF pores, and then hydrogen is introduced to reduce the organometallics or high temperature is applied to thermally decompose the precursors to form MNPs in the nanopores. Considering the relatively complex conditions of the CVD technique, a simple solid grinding approach to load metal precursors into MOFs was further developed.^[91–93] The volatile organometallic dimethyl Au(III) acetylacetonate, when being selected as a metal precursor, can be introduced into various types of MOFs, including MIL-53, MOF-5, HKUST-1, ZIF-8, etc., by solid grinding in air. Upon reduction in H₂ atmosphere at high temperature, Au NPs/MOF composites can be obtained.^[91] Surprisingly, this facile method led to the formation of MNPs with quite small sizes (around 2 nm), which exhibited high catalytic activity toward oxidation reactions.

Although the CVD and solid grinding methods have achieved good success, the precursors are limited to volatile species, and some volatile organometallic precursors are expensive and sensitive to air/water. This problem can be well tackled by utilizing the liquid-phase impregnation method.^[94,95] In a typical synthesis, a porous MOF is immersed in the solution containing the metal precursors, usually in the form of chloride or nitrate salts. The metal ions infiltrate into the MOF pores by capillary force and are subsequently reduced to yield the deposited MNPs by a reducing agent, typically hydrogen or sodium borohydride.

A general drawback of liquid-phase impregnation method is the difficulty in the precise control of MNPs on the external surface of or inside the MOF crystals. To address this issue, Xu and co-workers developed a double solvent approach (DSA), in which the quantitative (less than MOF pore volume) metal precursor aqueous solution is fully incorporated into the hydrophilic pore environment of the host MOF based on capillary force and hydrophilic interaction, while an excess of organic solvent merits the good dispersion of the MOF with the metal precursor solution. The complete encapsulation of metal precursors into MOF pores guarantees the formation of MNPs inside MOF crystals upon subsequent reduction, thus minimizing the outside deposition of MNPs.^[96–101] The desolvated MIL-101 was first dispersed in a hydrophobic solvent (hexane) through ultrasonication, then a hydrophilic solvent (water) containing H₂PtCl₆ with a volume set equal to or less than the pore volume of MIL-101 was pumped into the above hexane with dispersed MIL-101.^[96] The limited volume of H₂PtCl₆ aqueous solution can be completely absorbed into the MIL-101 cavities by capillary force. The large amount of hydrophilic internal pore surface plays a critical role to facilitate the impregnation process. The synthesized sample was treated in a flow of H₂/He to afford Pt NPs with an average size of 1.8 ± 0.2 nm well encapsulated in MIL-101. The resulting Pt@MIL-101 represented high activity for liquid-phase ammonia borane hydrolysis, solid-phase ammonia borane thermal dehydrogenation, and gas-phase CO oxidation. In contrast to the traditional impregnation process, such DSA is very effective and almost no MNPs deposited on the external surface of MOF. The same group

further developed a strategy combining DSA with liquid-phase concentration-controlled reduction to successfully immobilize AuNi alloy NPs to MIL-101, showing excellent catalytic activity for NH₃BH₃ hydrolysis. The Pd@MIL-101, synthesized via the DSA method, exhibited excellent catalytic performance in the tandem dehydrogenation of ammonia borane and subsequent reduction of nitro compounds.^[99] Not limited to monometallic NPs, bimetallic PdAg alloy NPs (1.5 nm) were successfully obtained in the cavities of MIL-101 via DSA by Jiang and co-workers.^[100] The resultant PdAg@MIL-101 presented great catalytic activity and selectivity toward one-pot cascade reactions, on the basis of the integration of host–guest cooperation and bimetallic synergy, in which MIL-101 offers Lewis acidity and Pd affords hydrogenation activity while Ag increases selectivity to the expected product. In addition to bimetallic alloy NPs, the same group intentionally fabricated Pd@Co core–shell and PdCo alloy NPs inside a MOF by the rational selection of a suitable reduction agent.^[101] The obtained Pd@Co@MIL-101 catalyst possesses superior catalytic activity and especially excellent cyclic stability in hydrolytic dehydrogenation of NH₃BH₃. Ultrafine Pd NPs immobilized within the cavities of MIL-101 using DSA showed high activity and selectivity for the hydrodeoxygenation of vanillin, while the Pd NPs, with larger particle sizes, on the outer surface of MIL-101 exhibited lower activity and different selectivity. The high catalytic performance has been attributed to the nanoconfinement effect and strong interactions between reactants and confined Pd NPs, which is a good example showing the significance of size/location of MNPs immobilized to nanoporous materials.^[98]

Another approach, known as “bottle-around-ship” or templated synthetic approach, involves the synthesis of MNPs first and subsequent addition of suitable reactants to assemble the MOF around the MNPs. By using this method, the aggregation of MNPs on the MOF external surface in the above approach can be effectively avoided. Moreover, the size, composition and shape of incorporated MNPs can be easily controlled. Lu et al. reported a controlled coating approach for encapsulation of the polyvinylpyrrolidone (PVP)-stabled NPs with various sizes, shapes and compositions into ZIF-8 (**Figure 7a**).^[102] The spatial distribution of incorporated NPs within ZIF-8 crystals is also controllable by their addition sequence. This assembly method was successfully extendable to other nanostructured materials whose surfaces were modified by PVP. The sample of Pt/PVP/ZIF-8 was used for hydrogenation reaction, showing partially hydrogenated the *n*-hexene and completely inactive towards *trans*-2-hexene, which proved the size selectivity of MOFs and complete encapsulation of Pt NPs. In their following study, this method was further extended to the encapsulation of MNPs into other types of MOFs such as ZIF-7, MIL-53 and MIL-101-NH₂.^[103] Yaghi and co-workers used the similar approach to incorporate Pt NPs into UiO-66 structured MOF, and found that the chemical environment, which is endowed by the great tailorability of MOF, around Pt NPs played a critical role in the catalytic selectivity and activity in the gas-phase conversion of methylcyclopentane to acyclic isomer, olefins, cyclohexane, and benzene.^[104] Recently, Jiang and co-workers rationally grew ZIF-8 on presynthesized Pd nanocubes to obtain core–shell-structured Pd@ZIF-8 composites.^[105] Benefiting from the synergetic effect between Pd nanocube cores (active sites

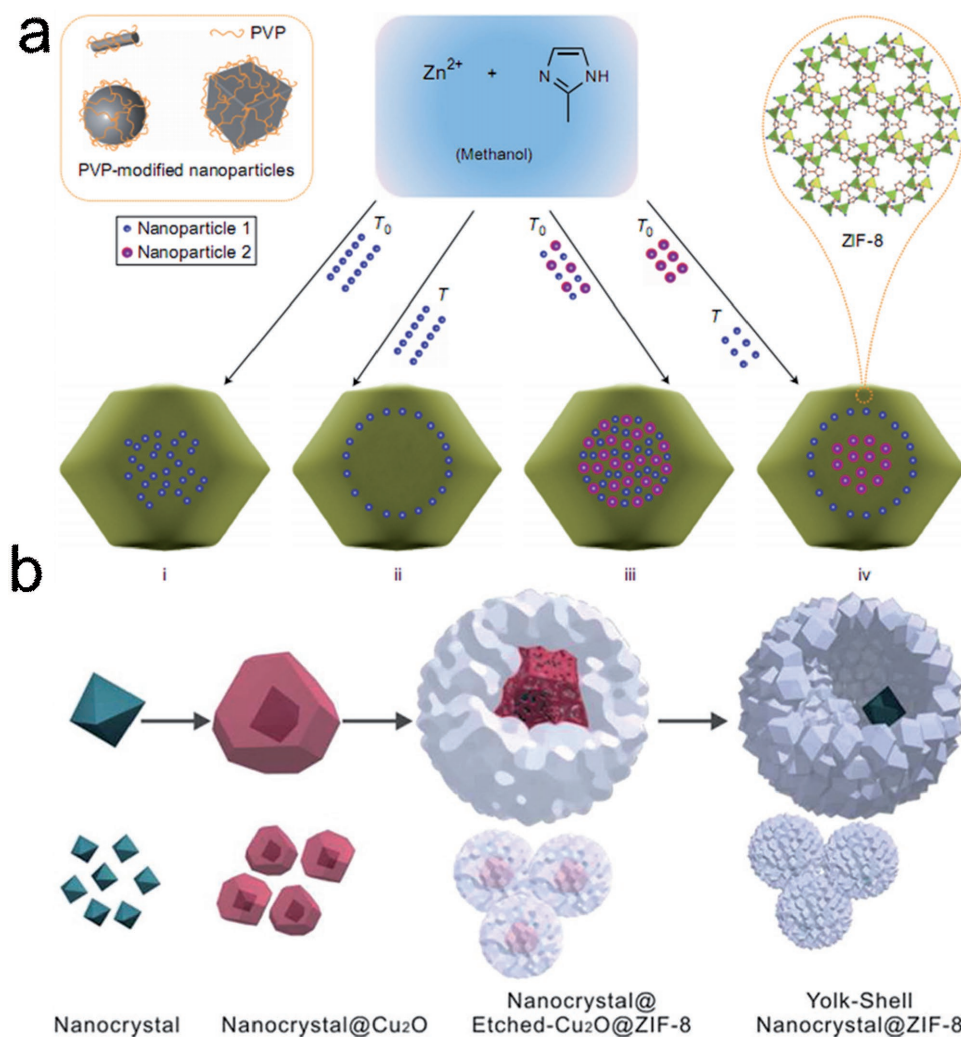


Figure 7. a,b) Schematic illustrations showing the controlled encapsulation of nanoparticles inside the controlled position of ZIF-8 particles (a), and the growth procedure for the nanocrystal@ZIF-8 yolk-shell nanostructures (b). a) Reproduced with permission.^[102] Copyright 2012, Nature Publishing Group. b) Reproduced with permission.^[106] Copyright 2012, American Chemical Society.

and plasmon-driven photothermal conversion) and ZIF-8 shell (H₂ enrichment, “molecular sieving” effect for substrates, and stabilization of Pd cores), Pd@ZIF-8 composites showed efficient, selective and recyclable catalytic hydrogenation of olefins at room temperature under 1 atm H₂ under light irradiation. Most importantly, this is, for the first time, the integration of the plasmonic photothermal effects of metal nanocrystals with MOFs for enhanced catalytic performance.

Yolk-shell structures of MNPs@MOF with a void between core and shell have also attracted board attention duo to their fascinating structures and tunable physical and chemical properties. Tsung and co-workers have created yolk-shell structured MNPs@MOF composites, for which the MNPs were first coated with a layer of Cu₂O as the sacrificial template and then a layer of polycrystalline ZIF-8 was grown (Figure 7b).^[106] The clean Cu₂O surface assisted in the formation of the ZIF-8 coating layer and was etched off spontaneously and simultaneously by the protons generated during the formation of ZIF-8. The yolk-shell nanostructures combine the functions

of nanoparticle cores, microporous shells, and a cavity in between, offering great potential in heterogeneous catalysis. Most recently, sandwich-like structured MOF/MNPs/MOF composites have also been graciously fabricated by Tang and co-workers via a stepwise synthetic strategy.^[107] In that work, the MOF serves as effective selectivity regulators by modulating the electron density of Pt active sites. Sandwiching Pt nanoparticles between an inner core with metal nodes of Cr³⁺ and an ultrathin outer shell with Fe³⁺ metal nodes, without affecting the diffusion of substrate evidently, results in stable catalysts that convert a range of α,β -unsaturated aldehydes with significantly enhanced selectivity towards unsaturated alcohols and high conversion efficiency.

In addition to the control of location of metal NPs relative to MOF support, which can be achieved by different approaches as described above, the morphology of metal NPs immobilized to MOFs can also be controlled. Xu and co-workers reported monometallic and bimetallic polyhedral metal nanocrystals, in the absence of surfactant protection, immobilized to MIL-101

by CO-directed reduction of metal precursors at the solid–gas interface.^[108] Pt cubes and Pd tetrahedra were formed by CO preferential bindings on their (100) and (111) facets, respectively, while PtPd bimetallic nanocrystals showed metal segregation, leading to Pd-rich core and Pt-rich shell.

2.3.4. Other Active Species

Different molecules such as organic dyes, enzymes, chiral molecules, and other functional molecules have also been composited with MOFs for catalysis. Taking advantage of the powerful confinement effect of MOFs, the use of them as encapsulators is proposed to be an efficient way to protect the incorporated molecules from aggregation, heterogeneous distribution and leaching. Liu et al. synthesized two hierarchically porous MOFs functionalized with carboxylic acid groups encapsulating a chiral molecule, (S)-2-(dimethylaminomethyl) pyrrolidine.^[109] After encapsulating the organic amine, the mesoporous framework was performed as an efficient and recyclable heterogeneous catalyst in the asymmetric direct aldol reactions and exhibited markedly improved catalytic performance relative to its homogeneous counterpart. Inspired by natural biomineralization processes, Liang et al. developed a novel method to incorporate biomacromolecules (e.g., proteins, enzymes, DNA) into the mesoporous MOFs and found that ZIF-8 coated horseradish peroxidase was able to retain its catalytic activity even after being treated in extreme conditions (high temperature and organic solvents).^[110] Recently, different large molecules with respective functionalities, meso-tetra(4-sulfonatophenyl)porphyrin (TSPP), tris(2,2'-bipyridine) dichlororuthenium(II) ([Ru(bpy)₃]Cl₂), and tetra-amido macrocyclic ligand catalytic activators (TAML-NaFeB*, a catalyst for C–H bond activation), were incorporated into the modified PCN-777 to afford heterogeneous catalysts and exhibited sound catalytic performance, accordingly.^[111]

2.4. MOF Derivatives

As a class of crystalline porous material with diversified and tailorable structures, MOFs offer congenial conditions as precursors to prepare porous carbon-based materials or metal (oxide)/carbon nanocomposites via pyrolysis, and their porosity and long-range structural ordering can be partially preserved. Furthermore, the much enhanced stability of MOF derivatives makes them suitable catalysts for reactions under harsh reaction conditions, for example, the Fischer-Tropsch synthesis. Here, we would briefly review the MOF-derived materials for catalytic applications in heterogeneous organic reactions, including oxidation, hydrogenation, dehydrogenation, and Fischer-Tropsch reactions, etc. The MOFs derivatives for electrocatalysis, as their main application, will be particularly discussed in Section 4.

2.4.1. Catalytic Oxidation Reactions

The oxidation of different substrates such as alcohols, hydrocarbons, CO and others, are a sort of important reactions, and

efficient catalysts for these reactions are highly desired. The MOF-derived materials have been found to be widely used for oxidation catalysis.^[23–25] Jiang and co-workers employed a Co-based MOF, ZIF-67, as a self-template and precursor to afford Co-CoO@N-doped porous carbon nanocomposites via pyrolysis under N₂ atmosphere, exhibiting excellent catalytic activity toward the direct oxidation of alcohols to esters with 100% conversion and selectivity to methyl benzoate even after six consecutive runs.^[112] In addition, aerobic oxidation of alcohols can also be achieved by a copper and carbon nanocomposite (Cu@C), prepared by simple pyrolysis of Cu₃(BTC)₂. The resulting Cu@C catalyst exhibited high efficiency for a broad scope of substrates.^[113] Beyond alcohols, the oxidation of hydrocarbons and CO have also been catalyzed by using MOF-derived materials, obtained by pyrolysis of Co-MOF,^[114] MIL-125(Ti),^[115] MIL-45b,^[116] HKUST-1^[117] and so on.

2.4.2. Catalytic Reduction Reactions

MOF-derived materials also have been employed as heterogeneous catalysts for reduction reactions, such as unsaturated bonds hydrogenation, hydrogenation of diverse nitro compounds and so on. Li and co-workers found that Co@C-N materials derived from a Co-containing MOF presented high activity and selectivity in the hydrogenation of a variety of unsaturated bonds, including C=C, C≡C, N=O, and C=O bonds, with isopropyl alcohol in the absence of any base additives.^[118] The Cu₃(BTC)₂ was used as both sacrificial template and copper precursor to give Cu/Cu₂O composite for catalytic reduction of 4-nitrophenol (4-NP) to 4-aminophenol (4-AP) by NaBH₄.^[119] Recently, Jiang and co-workers synthesized γ-Fe₂O₃ nanoparticles well dispersed in porous carbon, via one-step pyrolysis of Fe-MIL-88A. The resultant product exhibits excellent catalytic activity, chemoselectivity and magnetic recyclability for the hydrogenation of diverse nitro compounds to their corresponding amines under mild conditions.^[120] They also obtained metal-free porous carbon-based materials upon pyrolysis of different MOF precursors including MOF-5, ZIF-8, and PCN-224 for the catalytic reduction of 4-NP to 4-AP, and found that the pyrrolic nitrogen species played an important role for the catalytic efficiency.^[121] Han and co-workers synthesized Ni/SiO₂ and Co/SiO₂ catalysts with an average metal particle sizes of less than 1 nm by using MOF and tetraethoxysilane (TEOS) as the precursors and exhibited excellent activity in the catalytic benzene hydrogenation to cyclohexane in liquid phase under solvent-free conditions.^[122]

2.4.3. Other Catalytic Reactions

In addition to the above oxidation and reduction reactions, MOF-derived nanocomposites have been used for many types of catalytic reactions, such as dehydrogenation reaction, Fischer-Tropsch (FT) synthesis, etc. By the pyrolysis of the Fe-BDC MOF, Basolite F300, highly dispersed iron carbides embedded in a matrix of porous carbon with very high iron loadings (>40 wt%) were achieved. The unique iron spatial confinement and the absence of large iron particles in the resultant catalysts minimize catalyst deactivation, resulting in highly active

and stable operation in the FT reaction. Control experiments demonstrated that the MOF-derived catalysts possess productivities, on a total catalyst weight basis, one order of magnitude higher than the benchmark catalysts, namely the well-known Ruhrchemie and Sasol catalysts, even when the MOF-based catalysts contain a lower amount of iron.^[123] Fe-MIL-88B was also pyrolyzed to highly active catalysts for FT synthesis. The pyrolysis of the MOFs yielded nanoparticles with a unique Fe₃O₄@ χ -Fe₅C₂ core-shell structure dispersed on carbon supports, which correlated well with the very high activity for FT synthesis.^[124]

3. MOFs for Photocatalysis

Serving as a new platform, MOFs are able to organize different components to achieve photoresponse, which have attracted increasing research interest for application in artificial photosynthesis.^[19,20,125–127] Due to structural diversity and tailorability, MOFs have some special advantages for photocatalysis in comparison with traditional photocatalysts. First, the highly porous and crystalline structure of MOFs can provide the unrestricted diffusion of substrates and products through their open channels, and shorten the transport distance of charge carriers to the pore surface for reactions, greatly suppressing the classical volume recombination of electron-hole. Secondly, the great crystallinity can avoid the structural defects that might produce recombination centers. Thirdly, large surface areas of MOFs make the enriched substrates readily accessible to high-density catalytic sites in well-defined porous structures. Particularly, the most important advantage of MOFs with respect to other inorganic materials is their diversified and tailorable structures, which means that it is possible to tune the performance of MOF photocatalysts by the selection of appropriate building blocks and/or regulation of particular functional groups for target structures. In this section, we would mostly focus on the latest developments of MOFs on light-driven energy conversion reactions including water splitting, CO₂ reduction, and organic reactions. The early reports on MOF photocatalysis were mainly focused on organic pollutant degradation. The related work was summarized by Guo and co-workers recently^[128] and thus are not included in this short review.

3.1. MOFs for Photocatalytic Water Splitting

Water splitting contains two half reactions, water reduction (generating H₂) and water oxidation (producing O₂). Between these two half reactions, hydrogen generation was the first and dominantly reported by MOF photocatalysts. Mori and co-workers reported MOFs as a cocatalyst by incorporating a photosensitizer of Ru(bpy)₃²⁺ into the porous MOF [Ru₂(*p*-BDC)₂]_{*n*} (*p*-BDC = *p*-benzenedicarboxylate) for photoreducing water to H₂.^[129] A water stable Zr-MOF (UiO-66) built from BDC linker and Zr₆(O)₄(OH)₄(CO₂)₁₄ SBUs was developed as a photocatalyst for hydrogen production in a mixed solution of methanol and water under UV light irradiation.^[130] After introduction of -NH₂ group into the UiO-66 framework, the resulting amino-functionalized MOF, NH₂-UiO-66, can expand its absorption band to visible region and the catalytic activity can be increased

clearly. By the similar strategy, a Ti-based MOF, NH₂-MIL-125(Ti), was reported as a visible-light-responsive photocatalyst for H₂ evolution with Pt NPs and triethanolamine (TEOA) as the cocatalyst and electron sacrificial agent, respectively.^[131] The influence of different noble metals (Pt and Au) decorated on NH₂-MIL-125(Ti) for photocatalytic performance has been studied under visible-light irradiation in saturated CO₂ in the presence of TEOA.^[132] Additionally, amine-functionalized MIL-101(Cr) was also reported for photocatalytic hydrogen production from water.^[133]

Although -NH₂ group modified MOFs were developed for H₂ generation from water splitting under visible light, the longest wavelength is limited to \approx 500 nm due to the weak visible response of BDC-NH₂. To harvest visible light more efficiently, it is highly desired to develop MOFs with photoresponse covering the visible region as widely as possible. Porphyrins, with ideal visible-light absorption covering almost the whole range of visible light, are attractive organic motifs to construct porphyrinic-based MOFs for photocatalysis. With this consideration, a water-stable Al-porphyrinic MOF as a photocatalyst for hydrogen generation from water splitting under visible light irradiation (Figure 8a),^[134] presenting a turnover number of 8.16 and a quantum yield of 4.82%.

Excepting for extending the scope of light adsorption, improving the efficiency of charge separation plays a vital

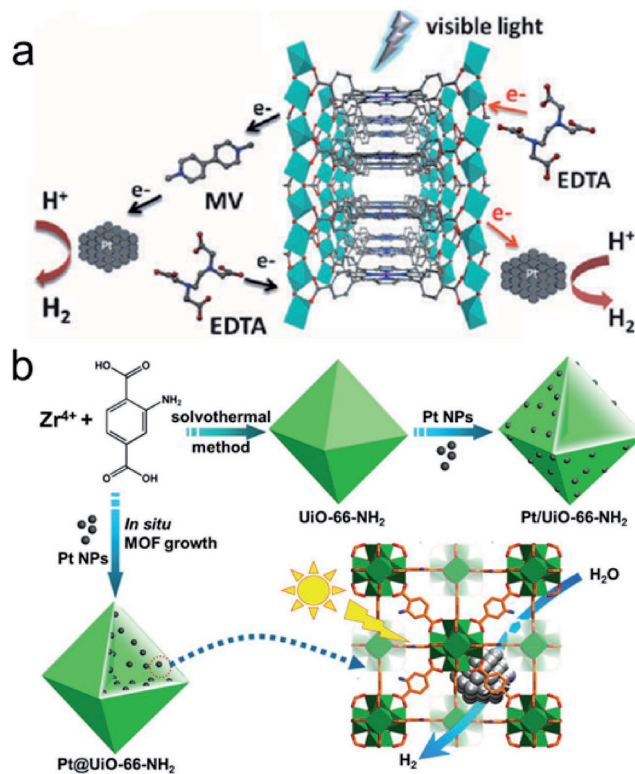


Figure 8. a) Proposed photocatalytic H₂ generation using Al-porphyrinic MOF in the presence of EDTA under visible light irradiation. Adapted with permission.^[134] Copyright 2012, Wiley-VCH. b) The synthesis of Pt@UiO-66-NH₂ and Pt/UiO-66-NH₂ with Pt NPs incorporated inside or supported on the MOF, respectively, for photocatalytic hydrogen production. Adapted with permission.^[136] Copyright 2016, Wiley-VCH.

importance role in photocatalysis. By the incorporation of cocatalyst, such as noble metal NPs, metal complexes, and POMs, more efficient charge separation can be achieved during the photocatalytic process. Lin and co-workers reported Pt@MOF composites with Pt NPs loaded into the cavities of the MOF. Being served as photocatalysts for hydrogen evolution, Pt@MOF composites showed high efficiency and high turnover number (TON).^[135] Recently, Jiang, Zhang and co-workers reported a photocatalyst of UiO-66-NH₂ incorporated with Pt NPs as electron acceptors for efficient H₂ production from water splitting under visible irradiation (Figure 8b).^[136] Moreover, results indicated that Pt NPs incorporated into MOFs with high dispersion, denoted as Pt@UiO-66-NH₂, exhibited a drastically enhanced activity about five times higher than Pt/UiO-66-NH₂, in which Pt NPs were well supported on MOFs, caused by the shorter path of electron transfer from MOFs to internal Pt and the surrounding environment of Pt NPs. Such a strategy to the improvement of MOF photocatalysis is not limited to MNPs, the combination of other active species and MOFs has been developed. Recently, a photocatalytic MOF UiO-66-[FeFe](dcbdt)(CO)₆ was synthesized via the incorporation of a molecular proton reduction catalyst [FeFe](dcbdt)(CO)₆ (dcbdt = 1,4-dicarboxylbenzene-2,3-dithiolate) into the framework of UiO-66 by the postsynthetic exchange strategy.^[137] The UiO-66-[FeFe](dcbdt)(CO)₆ showed an improved hydrogen production activity comparing with the reference catalysts, due to the synergistic effect the iron complex and the pristine UiO-66. The similar strategy was also reported in platinum complex modified MOF-253 for hydrogen production.^[138] Recently, Jiang and co-workers rationally encapsulated Co(II) complex (serving as electron acceptor and cocatalyst) into the cages of MIL-125-NH₂ in the absence of covalent binding between the two components and realized great catalytic efficiency for H₂ generation.^[139] POMs, involving multi redox active sites suitable for water-splitting, were also introduced into MOFs. Lin and co-workers embedded an anion [P₂W₁₈O₆₂]⁶⁻ into the cavities of a MOF via in situ self-assembly, and realized visible-light-driven proton reduction based on synergistic visible-light excitation of the MOFs and facile multi-electron injection to POM guests.^[140] Very recently, they reported Ni-containing POM [Ni₄(H₂O)₂(PW₉O₃₄)₂]¹⁰⁻ into [Ir(ppy)₂(bpy)]⁺-based UiO-MOF with the excellent photocatalytic activity for H₂ evolution.^[141]

In comparison with hydrogen production, less examples have been reported for photocatalytic water oxidation, probably due to the poor stability of most MOFs under water oxidation conditions (aqueous buffer solution, strong oxidant, etc.).^[126] In 2011, Lin and co-workers reported MOFs for water oxidation using cerium ammonium nitrate as an oxidant.^[142] Three iridium-based water oxidation catalysts, [Cp*Ir^{III}(dcpyp)Cl], [Cp*Ir^{III}(dcbpy)Cl]Cl, and [Ir^{III}(dcpyp)₂(H₂O)₂]OTf (dcpyp = 2-phenylpyridine-5,4'-dicarboxylic acid; dcbpy = 2,2'-bipyridine-5,5'-dicarboxylic acid) were incorporated into the framework of UiO-67. Compared to their homogeneous counterparts, the lower catalytic performance in oxygen evolution reaction over the obtained Ir-doped MOFs might be attributed to the difficult transport of the cerium(IV) oxidant throughout the small pores of the MOF. Subsequently, they prepared two other Zr-based MOFs with larger pore sizes using a longer Ir-based bridging ligand.^[143] Doping with two active Ir-based moieties,

both MOFs showed catalytic activities towards water oxidation, though partial decomposition of the iridium complexes was observed. Das and co-workers reported a stable MIL-101(Cr) for oxygen generation by incorporation of a molecular water oxidation catalyst, {[Mn(tpy)]₂(μ-O)₂}³⁺ (MnTD; tpy = 2,2':6',2''-terpyridine).^[144] The resulting composite exhibited slightly lower activity but much enhanced stability compared to the homogeneous catalyst, owing to the prevention of undesired intermolecular interaction between MnTD molecules. Recently, Fe-based MOFs were found to be promising candidates for efficient photocatalytic water oxidation by using [Ru(bpy)₃]²⁺ as a photosensitizer and Na₂S₂O₈ as an electron acceptor under visible light irradiation.^[145]

3.2. MOFs for Photocatalytic CO₂ Reduction

The efficient capture and catalytic transformation of CO₂ is a promising strategy to address excessive CO₂ emissions and global warming challenges induced by burning fossil fuels. MOFs have been extensively investigated and demonstrated significant advantages in selective CO₂ sorption during the past decade, owing to the high surface area of MOFs and their tunable interaction with CO₂ molecules. When serving as photocatalysts for CO₂ reduction, MOFs might effectively integrate the pre-concentration and transformation of CO₂ under visible-light irradiation, demonstrating their particular advantages for solar-light-induced CO₂ utilization. Li and co-workers realized NH₂-MIL-125(Ti) for photocatalytic CO₂ reduction under visible irradiation at a very early stage.^[146] Thanks to the introduction of amino-functionalized groups, NH₂-MIL-125(Ti) exhibited a higher photocatalytic activity than the parent MIL-125(Ti) (Figure 9a). The photocatalytic reduction of CO₂ into formate anion HCOO⁻ by Ti³⁺ in NH₂-MIL-125(Ti) was carried out in MeCN with TEOA as a sacrificial agent under visible light irradiation. Very recently, the same group developed a series of Fe-MOFs, Fe-MIL-101, Fe-MIL-53, Fe-MIL-88B, as active photocatalysts for reducing CO₂ to HCOO⁻ under visible light irradiation.^[147] Different from the previous MIL-125, the direct excitation of the Fe-oxo clusters in these Fe-MOFs induces the electron transfer from O²⁻ to Fe³⁺ to form Fe²⁺, which is responsible for the photocatalytic CO₂ reduction. Among the three Fe-MOFs, Fe-MIL-101 exhibited the highest activity due to the coordinatively unsaturated Fe centers involved. Thanks to the dual excitation pathways, all these three amine-functionalized Fe-MOFs showed enhanced activity of CO₂ photoreduction in comparison to the unfunctionalized MOFs. In addition, due to the great adaptability of MOFs structures, some mixed-ligand MOFs and/or mixed-metal MOFs have also been exploited for efficient photoreduction of CO₂.^[148]

Considering the insufficient visible light response of amine-modified MOFs, porphyrin motifs have been employed to construct MOFs for photocatalytic CO₂ reduction, due to their wide range of visible-light absorption. Liu et al. used porphyrinic MOF based on the coordination of porphyrinic carboxylate with Al³⁺ for photocatalytic conversion of CO₂ to methanol.^[149] They found that the presence of Cu²⁺ residing in the porphyrin center played an important role in improving the conversion efficiency via promoting the CO₂ chemical adsorption

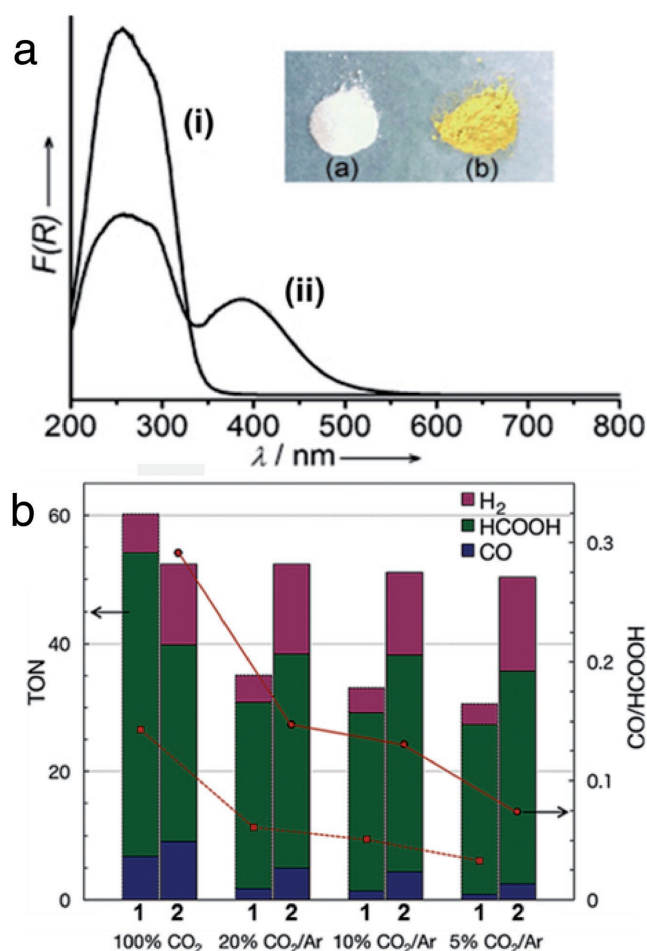


Figure 9. a) UV-vis spectra of i) MIL-125(Ti) and ii) NH₂-MIL-125(Ti). Inset: Photos showing the different colors of the two samples. Adapted with permission.^[146] Copyright 2012, Wiley-VCH. b) Photochemical reduction of CO₂ with [Ru^{II}(bpy)(terpy)(CO)](PF₆)₂ (1) (bpy = 2,2'-bipyridine, terpy = 2,2':6',2''-terpyridine) and PCP-Ru^{II} composite (2). Adapted with permission.^[154] Copyright 2016, Wiley-VCH.

and activation. Jiang and co-workers selected a very stable mesoporous Zr-porphyrinic MOF, PCN-222, for effective photoreduction of CO₂ to HCOO⁻, far superior to the porphyrin itself, under visible-light irradiation in the presence of TEOA as a sacrificial agent.^[150] The ultrafast transient absorption spectroscopy and time-resolved photoluminescence spectroscopy revealed an extremely long-lived electron trap state existed in PCN-222 to prevent the electron-hole recombination, thereby boosting the efficiency of CO₂ photoreduction, offering a deep understanding for efficient MOF photocatalysis. Recently, another Zr-porphyrinic MOF, MOF-525-Co, was also reported to selectively photoreduce CO₂ with high efficiency under visible-light irradiation. Mechanistic investigation reveals that the presence of single Co atoms in the porphyrin center can greatly boost the electron-hole separation efficiency for the MOF photocatalyst.^[151]

Though the pristine MOFs are potential for photocatalysis, the introduction of additional active sites greatly improves their catalytic activity. Many homogeneous molecular catalysts show high activity in photocatalytic CO₂ reduction, so it

is feasible to stabilize them inside MOFs to synergize their respective functions and thus boost the catalytic activity. Lin and co-workers reported a photocatalytic MOF, Zr₆(μ₃-O)₄(μ₃-OH)₄(bpdcc)_{5.83}(L₈)_{0.17} [bpdcc = 5,5'-biphenyldicarboxylate; H₂L₈ = ReI(CO)₃(5,5'-dcbpy)Cl], by incorporating the CO₂ photoreduction molecular catalyst ReI(CO)₃(5,5'-dcbpy)Cl into a UiO-67 framework for catalytic conversion of CO₂ to CO under visible irradiation.^[142] The TON of Re-complex-doped UiO-67 reached 10.9, three times higher than that of the homogeneous complex. Additionally, the use of homogeneous molecular catalysts as organic linkers to prepare corresponding MOF catalysts for CO₂ photoreduction was also reported. A MOF-253 supported active Ru carbonyl complex (MOF-253-Ru(CO)₂Cl₂) has been fabricated for photocatalytic CO₂ reduction under visible-light irradiation in a mixture of MeCN/TEOA.^[152] Recently, UiO-67 was subjected to postsynthetic modification to replace biphenyldicarboxylic acid with a rhodium complex, Cp^{*}Rh(bpydc)Cl₂ to achieve a rhodium-functionalized UiO-67 (Cp^{*}Rh@UiO-67).^[153] While the activity of the homogeneous and heterogeneous photocatalysts was comparable for CO₂ reduction, the Cp^{*}Rh@UiO-67 catalyst, even at low rhodium loading, was more stable and photocatalytically selective to formate. Furthermore, it can be recycled without loss of activity. Particularly, Kitagawa and co-workers reported a PCP-Ru^{II} catalyst with active Ru^{II}-CO complex for CO₂ reduction.^[154] With improved CO₂ adsorption behavior at ambient temperature, the PCP-Ru^{II} catalyst possess a high catalytic activity for CO₂ reduction to CO, HCOOH, and H₂. More importantly, in reference to the gradually reduced catalytic activity of the Ru^{II}-CO molecular catalyst under low CO₂ concentrations (diluted with Ar), the PCP-Ru^{II} displayed almost identical catalytic activity even at very low CO₂ concentrations (5% CO₂/Ar), highlighting the synergistic effect between the CO₂ adsorption and catalytically active sites within the PCP-Ru^{II} composite (Figure 9b).

The integration of molecular photosensitizers or semiconductor materials with MOFs have been reported to improve light absorption of MOFs or e-h separation, thus boosting CO₂ photoreduction. By incorporation of the negatively charged carbon nitride nanosheet (CNNS) with positively charged UiO-66, a facile electrostatic self-assembly method was developed to synthesize a UiO-66/CNNS photocatalyst, presenting much higher CO₂ photoreduction activity than bare CNNS and UiO-66/bulk CN counterparts.^[155] By using TiO₂ as the light-absorption unit and CPO-27-Mg as the CO₂ capture unit, a CPO-27-Mg/TiO₂ composite was also fabricated for CO₂ photoreduction under UV irradiation.^[156] A core-shell-structured HKUST-1@TiO₂ hybrid material was fabricated by coating TiO₂ shell onto HKUST-1 core, showing a fivefold enhancement in photocatalytic activity for the reduction of gaseous CO₂ to CH₄, as well as significantly promoted selectivity of CH₄ compared with the pristine TiO₂ photocatalyst.^[157] The ultrafast spectroscopy demonstrated that the photogenerated electrons were effectively transferred from TiO₂ to HKUST-1, facilitating charge separation in the semiconductor and supplying electrons to CO₂ adsorbed on the MOF. Not limited to semiconductors, molecular photosensitizers were also introduced to enhance photocatalytic activity of MOFs. A photosensitizer of [Ru(bpy)₃]Cl₂·6H₂O was immobilized into Co-ZIF-9 for excellent photoreduction of CO₂ to CO under visible-light irradiation.^[158] The

catalytic turnover number of Co-ZIF-9 reached 450 within 2.5 h and this original reactivity can be well maintained during prolonged operation under mild reaction conditions.

3.3. MOFs for Photocatalytic Organic Reactions

Upon light irradiation, photocatalysts can lead to efficient charge separation, which can be served to promote oxidation (reacting with photogenerated holes) and reduction (reacting with photogenerated electrons) of organic molecules, providing a novel methodology for the synthesis of fine chemicals. MOFs might be an ideal platform for photocatalytic organic reactions because of the semiconductor-like behavior with tunable band gap and the tailorable pores that facilitate the accessibility of high-density active sites and the transport of catalytic substrates/products. Based on the unique characters above, the utilization of MOFs as photocatalysts for catalytic organic transformations has attracted considerable research attention recently. Lin and co-workers incorporated metal complex, Ru(bpy)₃²⁺ or Ir(ppy)₂(bpy)⁺, into UiO-type MOFs to give photocatalysts for Aza-Henry reactions, oxidative coupling of amines and oxidation of sulfides.^[142] Though the resultant MOFs showed slightly lower activity compared to the homogeneous counterparts, their excellent reusability without decrease of activity can be achieved. Duan and co-workers developed a 3D CR-BPY1 MOF by solvothermal reaction of 4,4'-bipyridine (BPY), Cu(NO₃)₂·3H₂O and K₅[SiW₁₁O₃₉Ru(H₂O)]·10H₂O.^[159] The obtained CR-BPY1 integrated the [SiW₁₁O₃₉Ru(H₂O)]⁵⁻ photocatalyst and Cu catalyst and showed high photocatalytic activity and excellent size selectivity for the C–C coupling reaction of the *N*-phenyl-tetrahydroisoquinoline and nitromethane, suggesting that the catalytic reactions occurred in the MOF channels. The work demonstrated the example of merging the Cu catalysis and Ru photocatalysts in a single MOF to synergistically operate selective organic photosynthesis.

Oxidation reactions, as one of the most important reactions in the synthesis of fine chemicals, were widely investigated by MOFs. The metal 5,10,15,20-tetrakis(3,5-bis(carboxyl)phenyl) porphyrin (M-H₈TCPP) was chosen to construct a self-assembled metalloporphyrinic MOF, ZJU-18, exhibiting highly efficient and selective oxidation of ethylbenzene to acetophenone in quantitative >99% yield and a TON of 8076 after 48 h.^[160] NH₂-UiO-66 was also examined as a visible-light photocatalyst for selective aerobic oxygenation of various organic compounds including alcohols, olefins, and cycloalkanes, with high efficiency and high selectivity.^[161] NH₂-MIL-125(Ti) was investigated for photocatalytic aerobic oxidation of amines to imines under visible-light irradiation.^[162] A postsynthetic strategy to the fabrication of methyl red-functionalized MIL-125(Ti), extending the visible light absorption, was reported for the photocatalytic selective oxidation of benzyl alcohol to benzaldehyde in CH₃CN solution.^[163] Furthermore, MOF-based composites were also demonstrated for photocatalytic organic reactions, such as CdS-NH₂-UiO-66 nanocomposites for the selective oxidation of various alcohols by molecular oxygen under visible-light excitation,^[164] amorphous TiO₂ decorated HKUST-1 as the photocatalyst for the selective aerobic oxidation of 4-methylbenzyl alcohol to 4-methylbenzaldehyde with

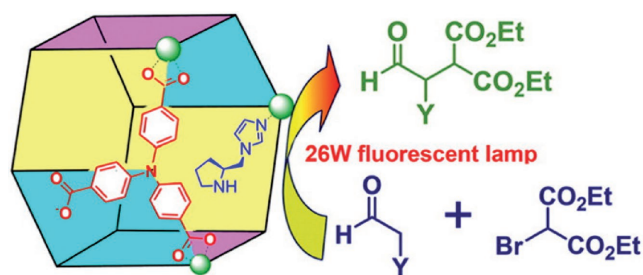


Figure 10. Schematic representation of Zn-PY11 for photocatalytic α -alkylation reaction upon light excitation. Reproduced with permission.^[166] Copyright 2012, American Chemical Society.

>93% selectivity and 89% conversion after 15 h light irradiation,^[165] etc.

Chiral MOFs are also good platforms for photocatalytic asymmetric reactions. A chiral organocatalyst [_L- or _D-pyrrolidine-2-ylimidazole (PYI)] and a photoactive unit (triphenylamine) were integrated into a single Zn-MOF, and a pair of MOF enantiomers were thus synthesized as asymmetric photocatalysts (**Figure 10**).^[166] Framework chirality was confirmed via single crystal crystallography and circular dichroism spectroscopy. The two MOFs proved to be efficient photocatalysts for the asymmetric α -alkylation of aliphatic aldehydes. Upon light excitation, the triphenylamine moiety within these MOFs induced electron transfer, and then produced an active intermediate for the photocatalytic α -alkylation reaction. Remarkably high enantioselectivities were achieved, and different chirality of the MOFs gave opposite selectivity.

4. MOFs for Electrocatalysis

Electrocatalytic system, mainly composing of oxygen reduction reaction (ORR), electrochemical water splitting (OER/HER), and electrochemical CO₂ reduction, is an alternative choice for renewable energy storage and conversion. To overcome the intrinsic high kinetic barriers in electrochemical process, noble-metal catalysts (e.g., Pt, Ir, Ru) are generally needed. Unfortunately, noble metals suffer from low abundance and high cost, impeding their industrial application. It is thus of great importance to develop earth-abundant alternatives with excellent activity and stability, such as heteroatom-doped carbon materials, transition metal/metal oxides, metal-containing compounds, etc.

Most MOFs are usually formed by first row transition metals (Fe, Co, Ni, Cu, Mn, etc.) and organic ligands mainly consist of C, H, O, N, etc. When being served as nonnoble metal electrocatalysts, MOFs offer several advantages, such as large surface area, tunable pore size and channels, designable structures, homogeneous dispersion of open active centers, and so on.^[23–27,167] However, the development of electrocatalysis for pure MOFs are usually restricted by their poor conductivity and instability in electrochemical systems. In view of this, MOFs have also been combined with conductive materials (carbon nanotube, graphene, etc.) to enhance their conductivity. Moreover, MOFs were served as ideal sacrificial templates to afford various nanostructured materials with both

high conductivity and stability, such as porous carbons, metal oxides, metal (oxides)/carbon composites, and other metal-containing compounds like metal carbides, metal nitrides, etc. The MOF-derived materials are able to inherit the advantages of pure MOFs to a certain degree, including high surface area, tailorable porosity, and easy functionalization with other heteroatoms or metal/metal oxides. These MOF derivatives not only greatly extend the catalytic application, but also avoid some crucial drawbacks of pristine MOFs. For example, MOF-derived nanostructures show much higher stability than pristine MOFs during electrochemical reaction even under harsh operating conditions (strong acidic or basic solution). On account of these advantages, MOF-based nanomaterials for electrocatalysis have received increasing attention in recent years.

4.1. MOFs for ORR

As described above, MOFs are able to provide very high surface areas with active metal centers. The high surface area ensures ease of access for O_2 species while active metal centers

are crucial for catalytic reaction. Pyridinium dye-functionalized reduced graphene oxide (G-dye) was employed as an excellent electron-conducting substrate to intercalate metalloporphyrin MOFs for the synthesis of MOF hybrids named as $(G\text{-dye-FeP})_n$, and the optimal composite of $(G\text{-dye } 50 \text{ wt\%-FeP})_n$ demonstrated high onset potential at -0.23 V versus Ag/AgCl in O_2 -saturated 0.1 M KOH solution with a four-electron transfer mechanism in ORR (Figure 11a).^[168]

Recently, extensive studies have shown that MOF carbonization offers an effective approach to the fabrication of desired structures and components for ORR. The MOF-derived metal/metal oxide-carbon nanohybrids (MMCs) could provide a good alternative to the Pt-based electrocatalysts for ORR. Among various transition metal-based MMCs systems, Co-N-C and Fe-N-C are important representatives from MOFs due to their high performance and excellent stability. Ma et al. reported the first example of MOF-derived material as the ORR catalyst.^[169] They selected a cobalt imidazolate framework as the initial candidate with the potential to produce high-density and regularly distributed catalytic centers of Co-N₄ moiety. The optimized catalyst showed an onset potential of 0.83 V versus a reversible

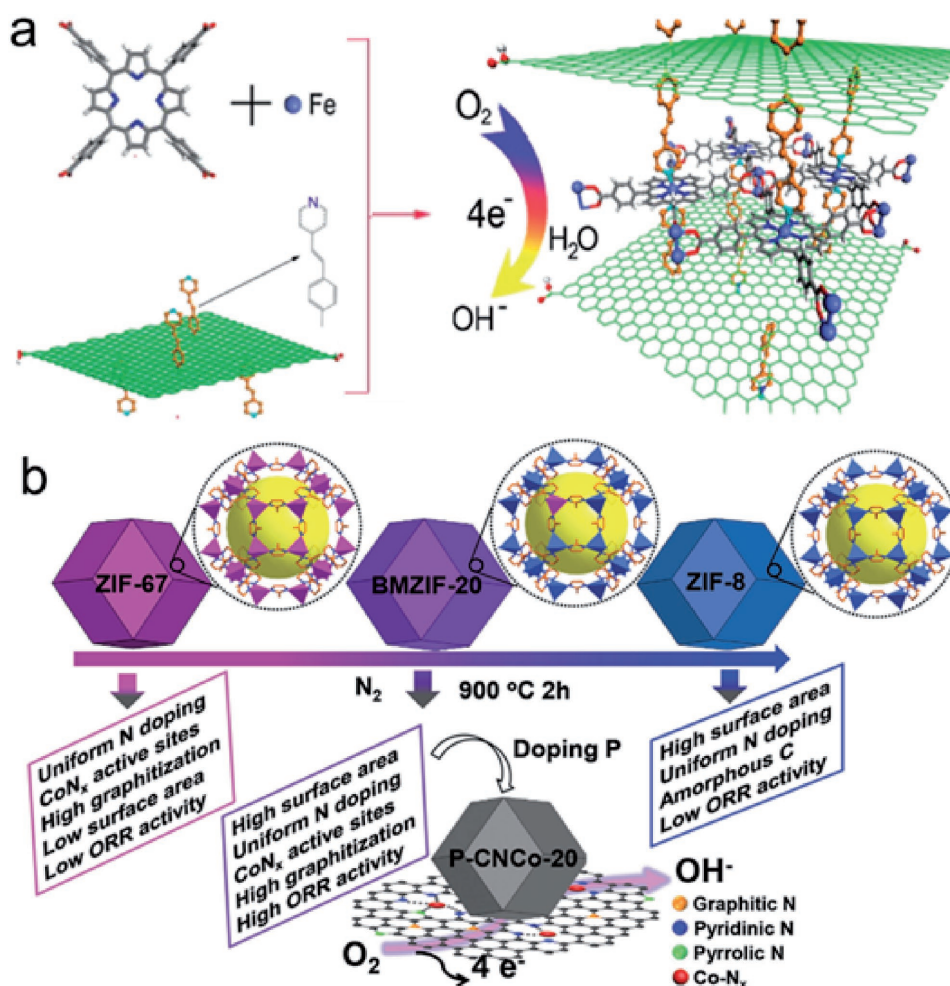


Figure 11. a) Schematic illustration showing the synthesis of $(G\text{-dye-FeP})_n$ by the assembly of rGO and G-dye. Adapted with permission.^[168] Copyright 2012, American Chemical Society. b) The preparation of doped porous carbons from BMZIFs for highly efficient oxygen reduction reaction. Reproduced with permission.^[177] Copyright 2015, Wiley-VCH.

hydrogen electrode (RHE), which was comparable to the best Co-based carbon catalysts. After that, ZIF-based electrocatalysts were widely investigated. Xu and co-workers synthesized N-decorated porous carbons with high surface areas using ZIF-8 as a template and precursor along with furfuryl alcohol and NH_4OH as the secondary carbon and nitrogen sources, respectively, which, with no metal species, exhibited excellent activity for ORR.^[170]

A typical ZIF material composed of $\text{Co}(\text{MeIm})_2$ primary units (MeIm = 2-methylimidazole), namely ZIF-67, was used directly as a precursor to prepare highly active Co–N–C ORR catalysts.^[171] Although the Co-ZIF-67-derived carbons have well-graphitized carbon matrix with active Co–N_x sites, they always show low surface area and porosity limiting the diffusion of electrolyte.^[171–174] On the contrary, the direct pyrolysis of Zn-based ZIF-8, which is isostructural with ZIF-67, can afford N-doped porous carbons with high-surface-area, whereas it cannot provide active Co–N_x sites and well-graphitized carbon.^[175,176] Bearing these in mind, Jiang and co-workers prepared a series of bimetallic ZIFs (BMZIFs) based on the lattice-matched ZIF-8 and ZIF-67 with varied Zn/Co ratios (Figure 11b).^[177] As expected, the obtained BMZIFs-derived porous carbons inherited the merits of the above two MOFs, which possessed large surface areas, high graphitization degree, and highly dispersed N and Co–N_x active species. The optimized Co/NC derived from BMZIF-20 (the Zn/Co molar ratio was 20) exhibited excellent ORR activity approaching the level of commercial Pt/C in alkaline media. Following a similar strategy, a couple of porous Co–N_x-C composites with excellent ORR catalytic properties have also been reported,^[178,179] manifesting the great promise of this Zn/Co bimetal MOF self-adjusted strategy for advanced electrodes in energy storage and conversion. In addition, some other strategies were also developed for MOF-based catalysts to enhance their ORR activity. Xia et al. introduced a highly ordered porous carbon matrix (CM) to grow Co-based ZIF-9.^[180] Combined with the porous matrix possessing interconnected ordered channels, the resultant $\text{Co}@\text{Co}_3\text{O}_4@\text{C-CM}$ showed almost identical ORR activity to the commercial Pt/C.

The Fe-based MOFs being another type of MOFs were widely investigated to derive active ORR catalysts with highly active Fe–N_x moieties. Li et al. reported different MOF-derived products of onion-like carbon NPs, N-doped carbon tubes, and N-doped graphene/graphene tubes synthesized at different pyrolysis temperatures.^[181] Among the products, the bamboo-like carbon nanotubes with trapped Fe_3C NPs inside the tubular structure exhibited an excellent ORR performance in both acidic and alkaline media. Tang and co-workers reported the direct pyrolysis of monodisperse nanoscale MIL-88B- NH_2 , formulated $\text{Fe}_3\text{O}(\text{NH}_2\text{-BTC})_3$, with controllable size and shape to produce a novel Fe- and N-codoped nanocarbon.^[182] The resultant composite exhibited excellent catalytic ORR activity in an alkaline system with an onset potential of 1.03 V and a half-wave potential of 0.92 V (vs RHE), which were better than those of the commercial Pt/C catalysts. A direct pyrolysis of GO-based Prussian blue (PB) nanocubes led to N-doped core-shell-structured porous $\text{Fe}/\text{Fe}_3\text{C}@\text{C}$ nanoboxes supported on reduced graphene oxide (rGO) nanosheets (denoted as N-doped $\text{Fe}/\text{Fe}_3\text{C}@\text{C}/\text{RGO}$), in which the PB nanocubes acted as templates/precursors and nitrogen sources.^[183] The N-doped

$\text{Fe}/\text{Fe}_3\text{C}@\text{C}/\text{RGO}$ showed far superior electrocatalytic activity with an onset potential of 1 V and a half-wave potential of 0.93 V (vs RHE), long-term stability, and methanol tolerance ability in reference to those of the commercial Pt/C catalyst, due to the synergistic effect between N-doped $\text{Fe}/\text{Fe}_3\text{C}@\text{C}$ and rGO. Hierarchically porous graphitic carbon architectures with atomically dispersed Fe and N doping were fabricated from a composite of MIL-101- NH_2 accommodating dicyandiamide (DCD) and FeCl_3 in the pore by using a facile strategy,^[184] which afforded high catalytic performance for ORR, outperforming the benchmark Pt catalyst and many state-of-the-art noble-metal-free catalysts in alkaline media, particularly in terms of the onset and half-wave potentials and durability. Such catalytic performance demonstrates the significant advantages of the unique hierarchically porous structure with efficient atomic doping, which provides a high density of accessible active sites for much improved mass and charge transports.

The MOF-derived metal sulfide–carbon nanohybrids, as another important type of ORR electrocatalysts, were also investigated due to their excellent activity and corrosion resistance. Recently, Zhu et al. reported N and S dual-doped honeycomb-like porous carbons with cobalt sulfide immobilized inside by a double-phase encapsulation approach and the subsequent guest-induced morphology control process.^[185] The resultant $\text{Co}_9\text{S}_8@\text{CNS900}$ derived from $\text{Co}(\text{II})\text{TU}@\text{MIL-101-NH}_2$ precursor exhibited comparable ORR activity to the commercial Pt/C under alkaline conditions.

In addition to plenty of metal-involved porous carbon composites mentioned above, single-metal atom catalysts are of great interest in catalysis. Based on the pyrolysis of a pre-designed bimetallic Zn/Co MOF, Li and co-workers reported a Co single atom/nitrogen-doped porous carbon (Co SAs/N–C) catalysts with high metal loading over 4 wt%, exhibiting excellent ORR reactivity.^[186] Via a cage encapsulated-precursor pyrolysis strategy, they also prepared a highly stable isolated single-atom iron (ISA Fe/CN) catalyst with Fe loading up to 2.16 wt%, presenting superior ORR performance than commercial Pt/C and most reported nonprecious metal catalysts.^[187] These findings open up a new avenue to the synthesis of MOF-derived single-atom metal catalysts.

4.2. MOFs for Water Splitting

In recent years, MOF-based materials have been exploited directly as electrocatalysts for water splitting. As early as 2011, Nohra et al. reported POM-based MOFs (POMOFs) as electrocatalysts for HER.^[188] Recently, Lan, Zhou and co-workers reported an ultrastable POMOF named NENU-500 as a robust HER electrocatalyst. Owing to the combination of the redox property of POM units and the porosity of MOFs, NENU-500 displayed a high activity for electrochemical hydrogen generation from water in 0.5 M H_2SO_4 , with a Tafel slope of 96 $\text{mV}\cdot\text{decade}^{-1}$ and an overpotential of 237 mV at a current density of 10 $\text{mA}\cdot\text{cm}^{-2}$, suggesting NENU-500 was a promising nonnoble metal electrocatalyst.^[189] Furthermore, the high HER activity of NENU-500 can also be maintained after 2000 cycles.

Recently, several robust MOFs have also been directly employed as OER catalysts for electrocatalytic water splitting.

Zhang, Li and co-workers reported a metal azolate framework [Co₂(μ-Cl)₂(bbta)] (MAF-X27-Cl, H₂bbta = 1*H*,5*H*-benzo-(1,2-*d*:4,5-*d'*)bistriazole) with ultrahigh stability in 1.0 M KOH.^[190] After replacing Cl⁻ of MAF-X27-Cl by OH⁻ group, the obtained [Co₂(μ-OH)₂(bbta)] (MAF-X27-OH), functionalized by open metal sites and hydroxide ligands, offered an overpotential of 292 mV at a current density of 10 mA·cm⁻², which was much better than most reported inorganic catalysts. In another work from Zhang's group, they skillfully immobilized and stabilized an unstable dicobalt cluster which is active for OER in a robust MOF skeleton named [Fe₃(μ₃-O)(bdc)₃(L^T)₃] (L^T = terminal ligand) and achieved exceptionally high OER activity.^[191] Tang and co-workers synthesized 2D NiCo bimetal-organic-framework nanosheets (NiCo-UMOFNs) for OER. Owing to the coupling effect between Co and Ni and the 2D ultrathin nanosheets morphology, NiCo-UMOFNs exhibited a very high OER activity and excellent stability.^[192]

In addition to pristine MOFs, MOF-derived nanomaterials were widely used as the promising nonnoble-metal electrocatalysts for the HER and OER. A two-step pyrolysis of H₃BO₃-containing ZIF-67 was developed to fabricate a hybrid of N,B-codoped graphitic carbon cages encapsulated Co NPs (denoted as Co@BCN) as a highly active and durable nonprecious metal electrocatalysts for HER in both acidic and alkaline media.^[193] The results revealed that the synergetic effect between the Co NPs and the N,B-codoped carbon shell played a key role in enhancing the HER catalytic performance of Co@BCN. Recently, a novel strategy was presented to Co₃O₄/NiCo₂O₄ double-shelled nanocages by annealing ZIF-67/Ni-Co layered double hydroxide nanocomposites in air.^[194] The obtained Co₃O₄/NiCo₂O₄ double-shelled nanocages exhibited high electrocatalytic activity and excellent stability for OER. In comparison to the MOF-derived porous carbon powders, the ordered array structures provide sufficient contact of catalytic active centers with the electrolyte, and also improve the diffusion of generated H₂ or O₂ away from the electrolyte during the HER or ORR. Based on this consideration, Qiao and co-workers reported an advanced 3D electrode based on porous Co₃O₄-carbon hybrids derived from MOF nanowire arrays grown on Cu foil without employing extra binders (**Figure 12a**).^[195] The derived structure of Co₃O₄-C composite retained the original nanowire morphology of the parent MOF with the addition of extra micro- and mesopores and showed an excellent OER activity, closing to the IrO₂/C noble metal catalyst. Most recently, Jiang, Yu and co-workers presented a versatile strategy for the controllable synthesis of 3D MOF hybrid arrays by utilizing semiconducting nanostructures as self-sacrificing templates. Particularly, MOF-hybrid-array-derived carbon-based composites with well-aligned hierarchical morphology and self-supporting structure can be directly applied to both anodes and cathodes for water splitting, displaying excellent electrocatalytic performance and being superior to the pristine semiconducting arrays, as well as other MOF-based counterparts.^[196]

Generally, for the practical application, the HER and OER should be conducted in the same electrolyte based on a single catalyst to achieve the overall water splitting. Recently, metal phosphides have attracted great attention due to unique chemical structure, higher stability, and wide application for overall water splitting. Dong and co-workers reported a porous CoP

electrocatalyst with a concave polyhedron structure derived from a Co-based MOF.^[197] To improve electrical conductivity and catalytic activity of MOF-derived nanomaterials, Jiang's group rationally designed sandwich-type ZIF-67/GO as a template and precursor to prepare layered CoP/rGO composites for HER and OER in alkaline media.^[198] The MOF-derived porous CoP guaranteed a large quantity of exposed active sites, and the close contact between CoP and rGO contributed to a continuous conductive network. When being employed as a bifunctional catalyst in both the anode and cathode for overall water splitting, CoP/rGO-400 showed superior performance to the integrated Pt/C and IrO₂ catalyst couple.

Considering the corrosion resistance, high stability and activity and low cost, molybdenum-based compounds become one of promising electrocatalysts for HER. A novel MOF-assisted strategy was developed to synthesize nanostructured MoC_x nanooctahedrons as the highly active electrocatalysts for HER, relying on the confined and in situ carburization of a Cu-based MOF (HKUST-1) as the host and template and Mo-based keggin POMs resided in MOF pores (**Figure 12b**).^[199] The as-prepared MoC_x nanooctahedrons consist of ultrafine nanocrystallites with an unusual η-MoC phase embedded in an amorphous carbon matrix, and possess a uniform and highly mesoporous structure. Benefiting from the porous and robust structure, the obtained MoC_x-based catalyst showed remarkable electrocatalytic activity for the HER with an onset potential of ≈25 mV (vs RHE) in acidic electrolyte and ≈80 mV (vs RHE) under basic conditions. Subsequently, the Cu-based POMOF/GO composite derived MoO₂@PC-RGO was prepared at a relatively low carbonization temperature.^[200] Thanks to the synergistic effect between highly dispersive MoO₂ particles and conductive rGO substrates, the obtained MoO₂@PC-RGO displayed excellent HER performance with a very positive onset potential close to Pt/C, low Tafel slope (41 mVdecade⁻¹), and remarkable long-term cycle stability in 0.5 M H₂SO₄.

4.3. MOFs for CO₂ Reduction

Though MOFs were widely used for CO₂ adsorption, separation and storage in the past decades, the potentials of MOF catalysts for CO₂ electroreduction were explored only in very recent years. Initially, the glass carbon electrode coated by a Cu-based MOF film, HKUST-1 or Cu₃(BTC)₂, was reported as electrocatalysts for CO₂ reduction reaction, during which electrochemically generated Cu(I) species played as Lewis acid to form adduct with adsorbed CO₂ and further transformed them into oxalic acid (H₂C₂O₄) as major product.^[201] In another case, a Cu-based MOF (CR-MOF) catalyst was used to reduce CO₂ into HCOOH with more positive onset potential than Cu metal electrode, proving that highly selective reduction of CO₂ was promising through rational design of MOFs.^[202]

Recently, a thin film of Fe-porphyrin-based MOF-253 (Fe-MOF-253) as a platform was adopted to anchor an electro-active Fe-porphyrin complexes on a conductive electrode for electrochemical reduction of CO₂ (**Figure 13a**).^[203] Thanks to the much denser active centers immobilized by MOF backbone on the surface of conductive electrode, the Fe-MOF-253 catalyst generated CO and H₂ as two major products in roughly equal

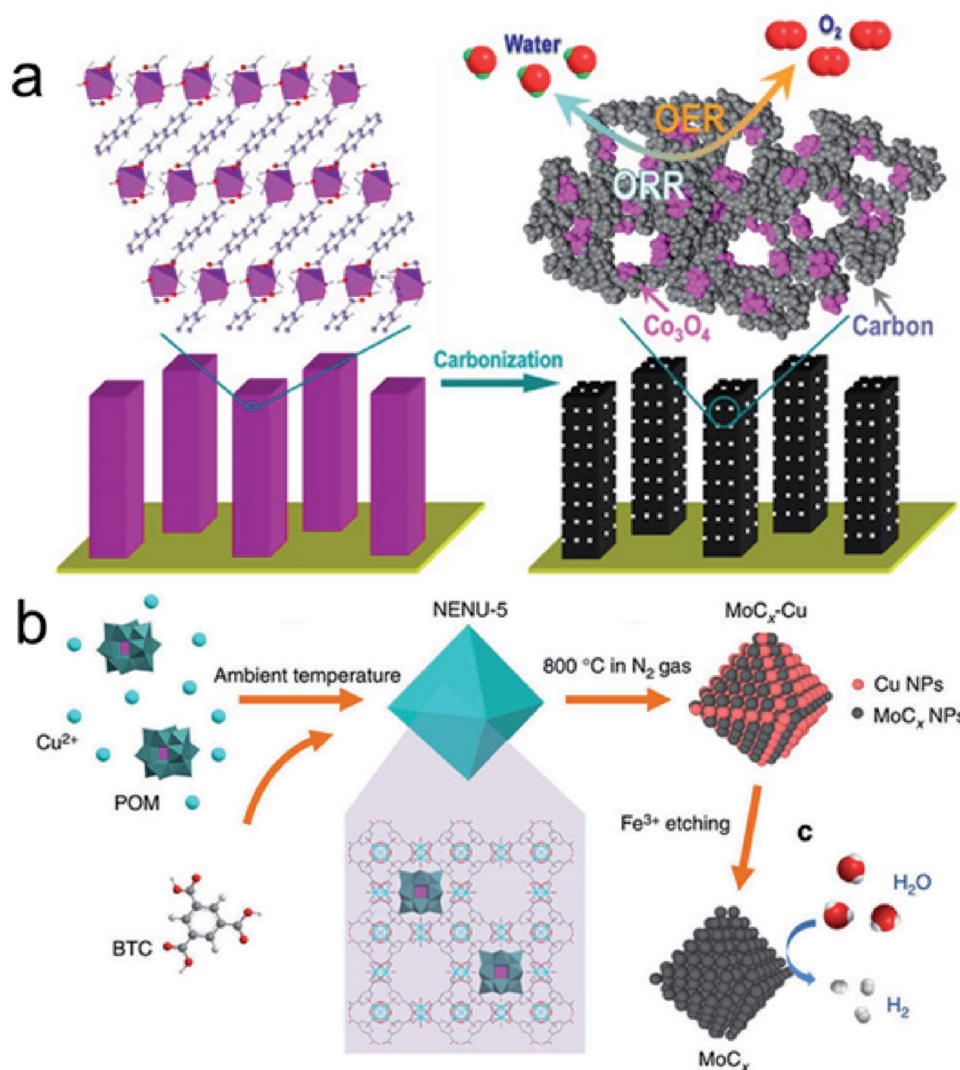


Figure 12. a) Schematic illustration showing the fabrication of $\text{Co}_3\text{O}_4\text{-C}$ nanowire arrays. Reproduced with permission.^[195] Copyright 2014, American Chemical Society. b) The synthetic procedure for porous MoC_x nanooctahedrons by a MOF-assisted strategy. Adapted with permission.^[199] Copyright 2015, Nature Publishing Group.

amount with much greater catalytic currents than the homogeneous catalyst, and the products provided a potential feedstock for Fisher–Tropsch synthesis of hydrocarbons. With a similar strategy, cobalt-porphyrin MOF ($\text{Al}_2(\text{OH})_2\text{TCPP-Co}$) thin films on a conductive substrate was used as robust catalysts for efficient and selective reduction of CO_2 to CO in aqueous electrolytes with a selectivity of 76% to CO and a per-site TON of 1400 (Figure 13b).^[204] In situ spectroelectrochemical measurements further indicated that the majority of catalytic centers were Co(I) reduced from Co(II) during the reaction. The above cases indicated that the integration of active species into MOFs might be an effective strategy toward the heterogenization of molecular catalysts for electrochemical CO_2 reduction with excellent performance. Additionally, recent studies revealed that the electrolyte type and the MOF morphology have significant effect on the selectivity and efficiency of CO_2 electroreduction reaction. For instance, the Zn-BTC MOF presented high selectivity of CH_4 using ionic liquids as the electrolytes.^[205] The sheet-like

Zn-MOF has the highest activity with a selectivity to CH_4 higher than 80% due to its largest electro-active surface areas.

5. Conclusions and Perspectives

In the past two decades, MOFs present impressive physicochemical properties with huge potential and special advantages in catalytic applications. Generally, pristine MOFs involve abundant coordinatively unsaturated metal sites (Lewis acid centers) and the active group on the organic linkers (usually acid/base sites), serving as acid or base catalysts, and MOFs are even able to integrate acid and base sites into one material simultaneously, presenting their unique characteristics for catalysis. In addition to the catalysis over pristine MOFs, people have further developed two main approaches that greatly expand the catalytic applications of MOFs by introducing active sites and/or particular functionalities.

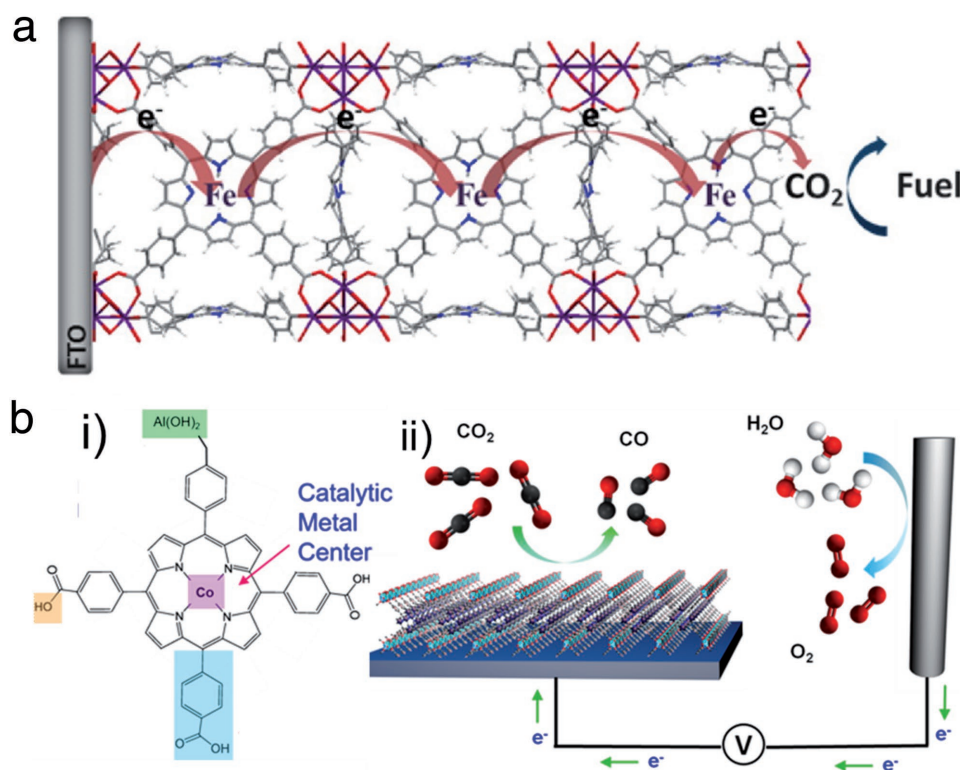


Figure 13. a) Schematic illustration of MOF-525 containing Fe porphyrins for electrochemical CO_2 reduction. Reproduced with permission.^[203] Copyright 2015, American Chemical Society. b) The cobalt-porphyrin MOF, $\text{Al}_2(\text{OH})_2\text{TCPP-Co}$ as electrocatalyst for CO_2 reduction (i: the organic building units, in the form of cobalt-metalated TCPP; ii: the functional CO_2 electrochemical reduction system integrated MOFs and a conductive substrate). Adapted with permission.^[204] Copyright 2015, American Chemical Society.

(a) Functionalized modification by grafting desired atoms/groups onto either metal ions/clusters or organic linkers. (b) Pore confinement/encapsulation of guest species, for example, metal complexes, enzyme, POMs, MNPs, etc. These two approaches greatly expand the catalytic reactions over MOFs and make them applicable in catalysis for a broad scope of reactions, by exerting respective functions of each component (MOF and additional atoms/groups/guest species) to realize “1 + 1 > 2” effect for enhanced catalysis. The MOF derivatives, with (partially) inherited porous character of MOFs, possess ultrahigh chemical and thermal stability and adjustable doping properties, and play distinctive role for catalysis, especially in reactions under harsh conditions. The troika of MOF-based materials, including pristine MOFs, functionalized MOFs and MOFs derivatives, have been demonstrated to be great potential in heterogeneous catalysis, including organocatalysis, photocatalysis, and electrocatalysis, etc.

Combining the merits of heterogeneous and homogeneous catalysts, MOFs have numerous advantages compared with the traditional catalysts: (i) the high dispersion and isolation of active sites maximize their utilization; (ii) diverse functional groups and/or active sites can be readily integrated into a single MOF for synergistic catalysis and cascade reactions; (iii) high porosity and surface area greatly facilitate the access of catalytic sites and substrate concentration; (iv) controllable pore size and tunable microenvironment around active sites are beneficial to the reaction activity and/or selectivity; (v) the well-defined MOF

structure merits the construction and understanding of the structure–property relationships, and so on.

Though tremendous advances have been achieved, MOF-based catalysts are currently in their infancy and more effort should be dedicated with the following concerns. (i) Highly stable MOFs with tailorable pore structures are everlasting targets, as stability guarantees the catalytic recyclability and pore size controls the mass transfer and size selectivity. (ii) The surrounding environment of active sites, including chirality, size, shape, electronic effect, etc., which is able to tune the interaction between active sites and substrate/products, a very crucial approach to the regulation of activity and selectivity,^[206–209] has not attracted sufficient attention. (iii) For MOF composites, most of the reports focus on confinement and size-selective effect. Unfortunately, the interaction between the host MOF and guest species, especially the electron interaction/transfer,^[210] which is of vital importance to modulate catalytic activity and selectivity, was rarely investigated and reported. (iv) The MOF-based photocatalysts always focus on the reduction reactions such as hydrogen evolution and CO_2 reduction with addition of electron sacrificial agent. To avoid the usage of sacrificial agent, the oxidation side reactions such as oxygen evolution are highly desired to be integrated with reduction reactions for practical consideration. (v) For MOF derivatives, due to their structural disorder, limited knowledge of the transformation mechanism restricts their rational fabrication. In situ experiments and/or advanced characterization techniques

would be introduced to further advance the understanding of this catalyst system.

In addition to the deliberate structural design for MOF-based catalysts to serve as ideal models for structure–property relationship investigation in laboratory, large-scale synthetic methods with high yields to afford low-cost MOFs are also necessary for practical applications. Currently, the catalytic reactions over MOFs are mostly probe reactions with conceptual explanations. In future, more important reactions that are closely related to the real industrial production should be explored in detail. With constant efforts toward those challenges, we believe that the MOFs will definitely present a bright future toward catalysis.

Acknowledgements

L.J. and Y.W. contributed equally to this work. This work was supported by the NSFC (Grant Nos. 21371162, 21673213, and 21521001), the National Research Fund for Fundamental Key Project (Grant No. 2014CB931803), the Recruitment Program of Global Youth Experts, Fundamental Research Funds for the Central Universities (Grant No. WK2060190065), JSPS, NEDO, and METI.

Conflict of Interest

The authors declare no conflict of interest.

Keywords

electrocatalysis, heterogeneous catalysis, metal–organic frameworks, photocatalysis

Received: June 30, 2017

Revised: August 15, 2017

Published online: November 27, 2017

- [1] H.-C. Zhou, J. R. Long, O. M. Yaghi, *Chem. Rev.* **2012**, *112*, 673.
- [2] H.-C. Zhou, S. Kitagawa, *Chem. Soc. Rev.* **2014**, *43*, 5415.
- [3] S. Ma, H.-C. Zhou, *Chem. Commun.* **2010**, *46*, 44.
- [4] B. Li, H.-M. Wen, Y. Cui, W. Zhou, G. Qian, B. Chen, *Adv. Mater.* **2016**, *28*, 8819.
- [5] L. E. Kreno, K. Leong, O. K. Farha, M. Allendorf, R. P. Van Duyne, J. T. Hupp, *Chem. Rev.* **2011**, *112*, 1105.
- [6] Z. Hu, B. J. Deibert, J. Li, *Chem. Soc. Rev.* **2014**, *43*, 5815.
- [7] T. Yamada, K. Otsubo, R. Makiura, H. Kitagawa, *Chem. Soc. Rev.* **2013**, *42*, 6655.
- [8] P. Horcajada, R. Gref, T. Baati, P. K. Allan, G. Maurin, P. Couvreur, G. Férey, R. E. Morris, C. Serre, *Chem. Rev.* **2011**, *112*, 1232.
- [9] M. Fujita, Y. J. Kwon, S. Washizu, K. Ogura, *J. Am. Chem. Soc.* **1994**, *116*, 1151.
- [10] D. Farrusseng, S. Aguado, C. Pinel, *Angew. Chem., Int. Ed.* **2009**, *48*, 7502.
- [11] J. Lee, O. K. Farha, J. Roberts, K. A. Scheidt, S. T. Nguyen, J. T. Hupp, *Chem. Soc. Rev.* **2009**, *38*, 1450.
- [12] A. Corma, H. García, F. Lladrés i Xamena, *Chem. Rev.* **2010**, *110*, 4606.
- [13] J. Liu, L. Chen, H. Cui, J. Zhang, L. Zhang, C.-Y. Su, *Chem. Soc. Rev.* **2014**, *43*, 6011.
- [14] Q.-G. Zhai, X. Bu, X. Zhao, D.-S. Li, P. Feng, *Acc. Chem. Res.* **2017**, *50*, 407.
- [15] X. Zhao, X. Bu, Q.-G. Zhai, H. Tran, P. Feng, *J. Am. Chem. Soc.* **2015**, *137*, 1396.
- [16] X. Zhao, X. Bu, E. T. Nguyen, Q.-G. Zhai, C. Mao, P. Feng, *J. Am. Chem. Soc.* **2016**, *138*, 15102.
- [17] H. Deng, C. J. Doonan, H. Furukawa, R. B. Ferreira, J. Towne, C. B. Knobler, B. Wang, O. M. Yaghi, *Science* **2010**, *327*, 846.
- [18] S. M. Cohen, *J. Am. Chem. Soc.* **2017**, *139*, 2855.
- [19] A. Dhakshinamoorthy, A. M. Asiri, H. García, *Angew. Chem., Int. Ed.* **2016**, *55*, 5414.
- [20] T. Zhang, W. Lin, *Chem. Soc. Rev.* **2014**, *43*, 5982.
- [21] B. Liu, H. Shioyama, T. Akita, Q. Xu, *J. Am. Chem. Soc.* **2008**, *130*, 5390.
- [22] H.-L. Jiang, B. Liu, Y.-Q. Lan, K. Kuratani, T. Akita, H. Shioyama, F. Zong, Q. Xu, *J. Am. Chem. Soc.* **2011**, *133*, 11854.
- [23] K. Shen, X. Chen, J. Chen, Y. Li, *ACS Catal.* **2016**, *6*, 5887.
- [24] J.-K. Sun, Q. Xu, *Energy Environ. Sci.* **2014**, *7*, 2071.
- [25] Y. V. Kaneti, J. Tang, R. R. Salunkhe, X. Jiang, A. Yu, K. C. W. Wu, Y. Yamauchi, *Adv. Mater.* **2017**, *29*, 1604898.
- [26] W. Xia, A. Mahmood, R. Zou, Q. Xu, *Energy Environ. Sci.* **2015**, *8*, 1837.
- [27] H. Wang, Q.-L. Zhu, R. Zou, Q. Xu, *Chem* **2017**, *2*, 52.
- [28] K. Schlichte, T. Kratzke, S. Kaskel, *Microporous Mesoporous Mater.* **2004**, *73*, 81.
- [29] L. Alaerts, E. Séguin, H. Poelman, F. Thibault-Starzyk, P. A. Jacobs, D. E. De Vos, *Chem. Eur. J.* **2006**, *12*, 7353.
- [30] A. Henschel, K. Gedrich, R. Kraehnert, S. Kaskel, *Chem. Commun.* **2008**, 4192.
- [31] S. Horike, M. Dinca, K. Tamaki, J. R. Long, *J. Am. Chem. Soc.* **2008**, *130*, 5854.
- [32] J. E. Mondloch, M. J. Katz, W. C. Isley Iii, P. Ghosh, P. Liao, W. Bury, G. W. Wagner, M. G. Hall, J. B. DeCoste, G. W. Peterson, R. Q. Snurr, C. J. Cramer, J. T. Hupp, O. K. Farha, *Nat. Mater.* **2015**, *14*, 512.
- [33] S. Y. Moon, Y. Liu, J. T. Hupp, O. K. Farha, *Angew. Chem., Int. Ed.* **2015**, *54*, 6795.
- [34] R.-Q. Zou, H. Sakurai, S. Han, R.-Q. Zhong, Q. Xu, *J. Am. Chem. Soc.* **2007**, *129*, 8402.
- [35] Z. Fang, B. Bueken, D. E. De Vos, R. A. Fischer, *Angew. Chem., Int. Ed.* **2015**, *54*, 7234.
- [36] F. Vermoortele, B. Bueken, G. Le Bars, B. Van de Voorde, M. Vandichel, K. Houthoofd, A. Vimont, M. Daturi, M. Waroquier, V. Van Speybroeck, C. Kirschhock, D. E. De Vos, *J. Am. Chem. Soc.* **2013**, *135*, 11465.
- [37] Z.-R. Jiang, H. Wang, Y. Hu, J. Lu, H.-L. Jiang, *ChemSusChem* **2015**, *8*, 878.
- [38] P. Horcajada, S. Surblé, C. Serre, D.-Y. Hong, Y.-K. Seo, J.-S. Chang, J.-M. Grenèche, I. Margiolakid, G. Férey, *Chem. Commun.* **2007**, *27*, 2820.
- [39] G. Chaplais, A. Simon-Masseron, F. Porcher, C. Lecomte, D. Bazer-Bachi, N. Bats, J. Patarin, *Phys. Chem. Chem. Phys.* **2009**, *11*, 5241.
- [40] M. H. Beyzavi, R. C. Klet, S. Tussupbayev, J. Borycz, N. A. Vermeulen, C. J. Cramer, J. F. Stoddart, J. T. Hupp, O. K. Farha, *J. Am. Chem. Soc.* **2014**, *136*, 15861.
- [41] G. Akiyama, R. Matsuda, H. Sato, M. Takata, S. Kitagawa, *Adv. Mater.* **2011**, *23*, 3294.
- [42] Y.-X. Zhou, Y.-Z. Chen, Y. Hu, G. Huang, S.-H. Yu, H.-L. Jiang, *Chem. Eur. J.* **2014**, *20*, 14976.
- [43] M. J. Ingleson, J. P. Barrio, J. Bacsca, C. Dickinson, H. Park, M. J. Rosseinsky, *Chem. Commun.* **2008**, *11*, 1287.
- [44] L. Zhu, X.-Q. Liu, H.-L. Jiang, L.-B. Sun, *Chem. Rev.* **2017**, *117*, 8129.
- [45] J. S. Seo, D. Whang, H. Lee, S. I. Jun, J. Oh, Y. J. Jeon, K. Kim, *Nature* **2000**, *404*, 982.

- [46] S. Hasegawa, S. Horike, R. Matsuda, S. Furukawa, K. Mochizuki, Y. Kinoshita, S. Kitagawa, *J. Am. Chem. Soc.* **2007**, *129*, 2607.
- [47] J. Gascon, U. Aktay, M. D. Hernandez-Alonso, G. P. van Klink, F. Kapteijn, *J. Catal.* **2009**, *261*, 75.
- [48] H. Liu, F.-G. Xi, W. Sun, N.-N. Yang, E.-Q. Gao, *Inorg. Chem.* **2016**, *55*, 5753.
- [49] F. Vermoortele, R. Ameloot, A. Vimont, C. Serre, D. De Vos, *Chem. Commun.* **2011**, *47*, 1521.
- [50] A. M. Shultz, O. K. Farha, J. T. Hupp, S. T. Nguyen, *J. Am. Chem. Soc.* **2009**, *131*, 4204.
- [51] O. K. Farha, A. M. Shultz, A. A. Sarjeant, S. T. Nguyen, J. T. Hupp, *J. Am. Chem. Soc.* **2011**, *133*, 5652.
- [52] C. Zou, T. Zhang, M.-H. Xie, L. Yan, G.-Q. Kong, X.-L. Yang, A. Ma, C.-D. Wu, *Inorg. Chem.* **2013**, *52*, 3620.
- [53] M.-H. Xie, X.-L. Yang, Y. He, J. Zhang, B. Chen, C.-D. Wu, *Chem. Eur. J.* **2013**, *19*, 14316.
- [54] D. Feng, Z.-Y. Gu, J.-R. Li, H.-L. Jiang, Z. Wei, H.-C. Zhou, *Angew. Chem., Int. Ed.* **2012**, *51*, 10307.
- [55] W. Morris, B. Voloskiy, S. Demir, F. Gándara, P. L. McGrier, H. Furukawa, D. Cascio, J. F. Stoddart, O. M. Yaghi, *Inorg. Chem.* **2012**, *51*, 6443.
- [56] Y. Chen, T. Hoang, S. Ma, *Inorg. Chem.* **2012**, *51*, 12600.
- [57] D. Feng, W.-C. Chung, Z. Wei, Z.-Y. Gu, H.-L. Jiang, Y.-P. Chen, D. J. Darensbourg, H.-C. Zhou, *J. Am. Chem. Soc.* **2013**, *135*, 17105.
- [58] S. H. Cho, B. Ma, S. T. Nguyen, J. T. Hupp, T. E. Albrecht-Schmitt, *Chem. Commun.* **2006**, *24*, 2563.
- [59] A. M. Shultz, O. K. Farha, D. Adhikari, A. A. Sarjeant, J. T. Hupp, S. T. Nguyen, *Inorg. Chem.* **2011**, *50*, 3174.
- [60] F. Song, C. Wang, J. M. Falkowski, L. Ma, W. Lin, *J. Am. Chem. Soc.* **2010**, *132*, 15390.
- [61] J. M. Falkowski, C. Wang, S. Liu, W. Lin, *Angew. Chem., Int. Ed.* **2011**, *50*, 8674.
- [62] C. Zhu, G. Yuan, X. Chen, Z. Yang, Y. Cui, *J. Am. Chem. Soc.* **2012**, *134*, 8058.
- [63] C.-D. Wu, A. Hu, L. Zhang, W. Lin, *J. Am. Chem. Soc.* **2005**, *127*, 8940.
- [64] K. Mo, Y. Yang, Y. Cui, *J. Am. Chem. Soc.* **2014**, *136*, 1746.
- [65] Y. K. Hwang, D. Y. Hong, J. S. Chang, S. H. Jhung, Y. K. Seo, J. Kim, A. Vimont, M. Daturi, C. Serre, G. Férey, *Angew. Chem., Int. Ed.* **2008**, *47*, 4144.
- [66] M. Banerjee, S. Das, M. Yoon, H. J. Choi, M. H. Hyun, S. M. Park, G. Seo, K. Kim, *J. Am. Chem. Soc.* **2009**, *131*, 7524.
- [67] D. Yang, S. O. Odoh, T. C. Wang, O. K. Farha, J. T. Hupp, C. J. Cramer, L. Gagliardi, B. C. Gates, *J. Am. Chem. Soc.* **2015**, *137*, 7391.
- [68] H. Noh, Y. Cui, A. W. Peters, D. R. Pahls, M. A. Ortuño, N. A. Vermeulen, C. J. Cramer, L. Gagliardi, J. T. Hupp, O. K. Farha, *J. Am. Chem. Soc.* **2016**, *138*, 14720.
- [69] Z. Li, N. M. Schweitzer, A. B. League, V. Bernales, A. W. Peters, A. B. Getsoian, T. C. Wang, J. T. Miller, A. Vjunov, J. L. Fulton, J. A. Lercher, C. J. Cramer, L. Gagliardi, J. T. Hupp, O. K. Farha, *J. Am. Chem. Soc.* **2016**, *138*, 1977.
- [70] K. Manna, P. Ji, Z. Lin, F. X. Greene, A. Urban, N. C. Thacker, W. Lin, *Nat. Commun.* **2016**, *7*, 12610.
- [71] P. Ji, K. Manna, Z. Lin, A. Urban, F. X. Greene, G. Lan, W. Lin, *J. Am. Chem. Soc.* **2016**, *138*, 12234.
- [72] E. D. Bloch, D. Britt, C. Lee, C. J. Doonan, F. J. Uribe-Romo, H. Furukawa, J. R. Long, O. M. Yaghi, *J. Am. Chem. Soc.* **2010**, *132*, 14382.
- [73] F. Carson, S. Agrawal, M. Gustafsson, A. Bartoszewicz, F. Moraga, X. Zou, B. Martín-Matute, *Chem. Eur. J.* **2012**, *18*, 15337.
- [74] M. Pintado-Sierra, A. M. Rasero-Almansa, A. Corma, M. Iglesias, F. Sánchez, *J. Catal.* **2013**, *299*, 137.
- [75] J. Canivet, S. Aguado, Y. Schuurman, D. Farrusseng, *J. Am. Chem. Soc.* **2013**, *135*, 4195.
- [76] M. H. Alkordi, Y. Liu, R. W. Larsen, J. F. Eubank, M. Eddaoudi, *J. Am. Chem. Soc.* **2008**, *130*, 12639.
- [77] R. W. Larsen, L. Wojtas, J. Perman, R. L. Musselman, M. J. Zaworotko, C. M. Vromvile, *J. Am. Chem. Soc.* **2011**, *133*, 10356.
- [78] E. Kockrick, T. Lescouet, E. V. Kudrik, A. B. Sorokin, D. Farrusseng, *Chem. Commun.* **2011**, *47*, 1562.
- [79] B. Li, Y. Zhang, D. Ma, T. Ma, Z. Shi, S. Ma, *J. Am. Chem. Soc.* **2014**, *136*, 1202.
- [80] D.-Y. Du, J.-S. Qin, S.-L. Li, Z.-M. Su, Y.-Q. Lan, *Chem. Soc. Rev.* **2014**, *43*, 4615.
- [81] S.-S. Wang, G.-Y. Yang, *Chem. Rev.* **2015**, *115*, 4893.
- [82] F.-J. Ma, S.-X. Liu, C.-Y. Sun, D.-D. Liang, G.-J. Ren, F. Wei, Y.-G. Chen, Z.-M. Su, *J. Am. Chem. Soc.* **2011**, *133*, 4178.
- [83] C.-Y. Sun, S.-X. Liu, D.-D. Liang, K.-Z. Shao, Y.-H. Ren, Z.-M. Su, *J. Am. Chem. Soc.* **2009**, *131*, 1883.
- [84] L. H. Wee, S. R. Bajpe, N. Janssens, I. Hermans, K. Houthoofd, C. E. Kirschhock, J. A. Martens, *Chem. Commun.* **2010**, *46*, 8186.
- [85] J. Song, Z. Luo, D. K. Britt, H. Furukawa, O. M. Yaghi, K. I. Hardcastle, C. L. Hill, *J. Am. Chem. Soc.* **2011**, *133*, 16839.
- [86] G. Cai, H.-L. Jiang, *Angew. Chem., Int. Ed.* **2017**, *56*, 563.
- [87] Q. Yang, Q. Xu, H.-L. Jiang, *Chem. Soc. Rev.* **2017**, *46*, 4774.
- [88] S. Hermes, M. K. Schröter, R. Schmid, L. Khodeir, M. Muhler, A. Tissler, R. W. Fischer, R. A. Fischer, *Angew. Chem., Int. Ed.* **2005**, *44*, 6237.
- [89] M. Meilikhov, K. Yusenko, R. A. Fischer, *J. Am. Chem. Soc.* **2009**, *131*, 9644.
- [90] M. Meilikhov, K. Yusenko, A. Torrisi, B. Jee, C. Mellot-Draznieks, A. Pöpl, R. A. Fischer, *Angew. Chem., Int. Ed.* **2010**, *49*, 6212.
- [91] T. Ishida, M. Nagaoka, T. Akita, M. Haruta, *Chem. Eur. J.* **2008**, *14*, 8456.
- [92] H.-L. Jiang, B. Liu, T. Akita, M. Haruta, H. Sakurai, Q. Xu, *J. Am. Chem. Soc.* **2009**, *131*, 11302.
- [93] H.-L. Jiang, Q.-P. Lin, T. Akita, B. Liu, H. Ohashi, H. Oji, T. Honma, T. Takei, M. Haruta, Q. Xu, *Chem. Eur. J.* **2011**, *17*, 78.
- [94] X. Gu, Z.-H. Lu, H.-L. Jiang, T. Akita, Q. Xu, *J. Am. Chem. Soc.* **2011**, *133*, 11822.
- [95] H.-L. Jiang, T. Akita, T. Ishida, M. Haruta, Q. Xu, *J. Am. Chem. Soc.* **2011**, *133*, 1304.
- [96] A. Aijaz, A. Karkamkar, Y. J. Choi, N. Tsumori, E. Rönnebro, T. Autrey, H. Shioyama, Q. Xu, *J. Am. Chem. Soc.* **2012**, *134*, 13926.
- [97] Q.-L. Zhu, J. Li, Q. Xu, *J. Am. Chem. Soc.* **2013**, *135*, 10210.
- [98] A. Aijaz, Q.-L. Zhu, N. Tsumori, T. Akita, Q. Xu, *Chem. Commun.* **2015**, *51*, 2577.
- [99] Q. Yang, Y.-Z. Chen, Z. U. Wang, Q. Xu, H.-L. Jiang, *Chem. Commun.* **2015**, *51*, 10419.
- [100] Y.-Z. Chen, Y.-X. Zhou, H. Wang, J. Lu, T. Uchida, Q. Xu, S.-H. Yu, H.-L. Jiang, *ACS Catal.* **2015**, *5*, 2062.
- [101] Y.-Z. Chen, Q. Xu, S.-H. Yu, H.-L. Jiang, *Small* **2015**, *11*, 71.
- [102] G. Lu, S. Li, Z. Guo, O. K. Farha, B. G. Hauser, X. Qi, Y. Wang, X. Wang, S. Han, X. Liu, J. S. DuChene, H. Zhang, Q. Zhang, X. Chen, J. Ma, S. C. J. Loo, W. D. Wei, Y. Yang, J. T. Hupp, F. Huo, *Nat. Chem.* **2012**, *4*, 310.
- [103] S. Li, F. Huo, *Small* **2014**, *10*, 4371.
- [104] K. M. Choi, K. Na, G. A. Somorjai, O. M. Yaghi, *J. Am. Chem. Soc.* **2015**, *137*, 7810.
- [105] Q. Yang, Q. Xu, S.-H. Yu, H.-L. Jiang, *Angew. Chem., Int. Ed.* **2016**, *55*, 3685.
- [106] C.-H. Kuo, Y. Tang, L.-Y. Chou, B. T. Sneed, C. N. Brodsky, Z. Zhao, C.-K. Tsung, *J. Am. Chem. Soc.* **2012**, *134*, 14345.
- [107] M. Zhao, K. Yuan, Y. Wang, G. Li, J. Guo, L. Gu, W. Hu, H. Zhao, Z. Tang, *Nature* **2016**, *539*, 76.

- [108] A. Aijaz, T. Akita, N. Tsumori, Q. Xu, *J. Am. Chem. Soc.* **2013**, *135*, 16356.
- [109] Y. Liu, X. Xi, C. Ye, T. Gong, Z. Yang, Y. Cui, *Angew. Chem., Int. Ed.* **2014**, *53*, 13821.
- [110] K. Liang, R. Ricco, C. M. Doherty, M. J. Styles, S. Bell, N. Kirby, S. Mudie, D. Haylock, A. J. Hill, C. J. Doonan, P. Falcaro, *Nat. Commun.* **2015**, *6*, 7240.
- [111] D. Feng, K. Wang, J. Su, T.-F. Liu, J. Park, Z. Wei, M. Bosch, A. Yakovenko, X. Zou, H.-C. Zhou, *Angew. Chem., Int. Ed.* **2015**, *54*, 149.
- [112] Y.-X. Zhou, Y.-Z. Chen, L. Cao, J. Lu, H.-L. Jiang, *Chem. Commun.* **2015**, *51*, 8292.
- [113] B. R. Kim, J. S. Oh, J. Kim, C. Y. Lee, *Catal. Lett.* **2016**, *146*, 734.
- [114] C. Bai, X. Yao, Y. Li, *ACS Catal.* **2015**, *5*, 884.
- [115] N. D. McNamara, J. Kim, J. C. Hicks, *Energy Fuels* **2016**, *30*, 594.
- [116] R. Fang, R. Luque, Y. Li, *Green Chem.* **2016**, *18*, 3152.
- [117] H. Tan, C. Ma, L. Gao, Q. Li, Y. Song, F. Xu, T. Wang, L. Wang, *Chem. Eur. J.* **2014**, *20*, 16377.
- [118] J. Long, Y. Zhou, Y. Li, *Chem. Commun.* **2015**, *51*, 2331.
- [119] H. Niu, S. Liu, Y. Cai, F. Wu, X. Zhao, *Microporous Mesoporous Mater.* **2016**, *219*, 48.
- [120] Y. Li, Y.-X. Zhou, X. Ma, H.-L. Jiang, *Chem. Commun.* **2016**, *52*, 4199.
- [121] G. Huang, L. Yang, X. Ma, J. Jiang, S.-H. Yu, H.-L. Jiang, *Chem. Eur. J.* **2016**, *22*, 3470.
- [122] X. Kang, H. Liu, M. Hou, X. Sun, H. Han, T. Jiang, Z. Zhang, B. Han, *Angew. Chem., Int. Ed.* **2016**, *55*, 1080.
- [123] V. P. Santos, T. A. Wezendonk, J. J. D. Jaén, A. I. Dugulan, M. A. Nasalevich, H.-U. Islam, A. Chojecki, S. Sartipi, X. Sun, A. A. Hakeem, A. C. J. Koeken, M. Ruitenbeek, T. Davidian, G. R. Meima, G. Sankar, F. Kapteijn, M. Makkee, J. Gascon, *Nat. Commun.* **2015**, *6*, 6451.
- [124] B. An, K. Cheng, C. Wang, Y. Wang, W. Lin, *ACS Catal.* **2016**, *6*, 3610.
- [125] J.-L. Wang, C. Wang, W. Lin, *ACS Catal.* **2012**, *2*, 2630.
- [126] S. Wang, X. Wang, *Small* **2015**, *11*, 3097.
- [127] K. Meyer, M. Ranocchiari, J. A. van Bokhoven, *Energy Environ. Sci.* **2015**, *8*, 1923.
- [128] C.-C. Wang, J.-R. Li, X.-L. Lv, Y.-Q. Zhang, G. Guo, *Energy Environ. Sci.* **2014**, *7*, 2831.
- [129] Y. Kataoka, K. Sato, Y. Miyazaki, K. Masuda, H. Tanaka, S. Naito, W. Mori, *Energy Environ. Sci.* **2009**, *2*, 397.
- [130] C. Gomes Silva, I. Luz, F. X. Llabrés i Xamena, A. Corma, H. García, *Chem. Eur. J.* **2010**, *16*, 11133.
- [131] Y. Horiuchi, T. Toyao, M. Saito, K. Mochizuki, M. Iwata, H. Higashimura, M. Anpo, M. Matsuoka, *J. Phys. Chem. C* **2012**, *116*, 20848.
- [132] D. Sun, W. Liu, Y. Fu, Z. Fang, F. Sun, X. Fu, Y. Zhang, Z. Li, *Chem. Eur. J.* **2014**, *20*, 4780.
- [133] M. Wen, K. Mori, T. Kamegawa, H. Yamashita, *Chem. Commun.* **2014**, *50*, 11645.
- [134] A. Fateeva, P. A. Chater, C. P. Ireland, A. A. Tahir, Y. Z. Khimiyak, P. V. Wiper, J. R. Darwent, M. J. Rosseinsky, *Angew. Chem., Int. Ed.* **2012**, *124*, 7558.
- [135] C. Wang, K. E. deKrafft, W. Lin, *J. Am. Chem. Soc.* **2012**, *134*, 7211.
- [136] J.-D. Xiao, Q. Shang, Y. Xiong, Q. Zhang, Y. Luo, S.-H. Yu, H.-L. Jiang, *Angew. Chem., Int. Ed.* **2016**, *55*, 9389.
- [137] S. Pullen, H. Fei, A. Orthaber, S. M. Cohen, S. Ott, *J. Am. Chem. Soc.* **2013**, *135*, 16997.
- [138] T. Zhou, Y. Du, A. Borgna, J. Hong, Y. Wang, J. Han, W. Zhang, R. Xu, *Energy Environ. Sci.* **2013**, *6*, 3229.
- [139] Z. Li, J.-D. Xiao, H.-L. Jiang, *ACS Catal.* **2016**, *6*, 5359.
- [140] Z.-M. Zhang, T. Zhang, C. Wang, Z. Lin, L.-S. Long, W. Lin, *J. Am. Chem. Soc.* **2015**, *137*, 3197.
- [141] X. J. Kong, Z. Lin, Z. M. Zhang, T. Zhang, W. Lin, *Angew. Chem., Int. Ed.* **2016**, *55*, 6411.
- [142] C. Wang, Z. Xie, K. E. deKrafft, W. Lin, *J. Am. Chem. Soc.* **2011**, *133*, 13445.
- [143] C. Wang, J.-L. Wang, W. Lin, *J. Am. Chem. Soc.* **2012**, *134*, 19895.
- [144] B. Nepal, S. Das, *Angew. Chem., Int. Ed.* **2013**, *52*, 7224.
- [145] L. Chi, Q. Xu, X. Liang, J. Wang, X. Su, *Small* **2016**, *12*, 1351.
- [146] Y. Fu, D. Sun, Y. Chen, R. Huang, Z. Ding, X. Fu, Z. Li, *Angew. Chem., Int. Ed.* **2012**, *51*, 3364.
- [147] D. Wang, R. Huang, W. Liu, D. Sun, Z. Li, *ACS Catal.* **2014**, *4*, 4254.
- [148] Y. Lee, S. Kim, J. K. Kang, S. M. Cohen, *Chem. Commun.* **2015**, *51*, 5735.
- [149] Y. Liu, Y. Yang, Q. Sun, Z. Wang, B. Huang, Y. Dai, X. Qin, X. Zhang, *ACS Appl. Mater. Interfaces* **2013**, *5*, 7654.
- [150] H.-Q. Xu, J. Hu, D. Wang, Z. Li, Q. Zhang, Y. Luo, S.-H. Yu, H.-L. Jiang, *J. Am. Chem. Soc.* **2015**, *137*, 13440.
- [151] H. Zhang, J. Wei, J. Dong, G. Liu, L. Shi, P. An, G. Zhao, J. Kong, X. Wang, X. Meng, J. Zhang, J. Ye, *Angew. Chem., Int. Ed.* **2016**, *55*, 14310.
- [152] D. Sun, Y. Gao, J. Fu, X. Zeng, Z. Chen, Z. Li, *Chem. Commun.* **2015**, *51*, 2645.
- [153] M. B. Chambers, X. Wang, N. Elgrishi, C. H. Hendon, A. Walsh, J. Bonnefoy, J. Canivet, E. A. Quadrelli, D. Farrusseng, C. Mellot-Draznieks, M. Fontecave, *ChemSusChem* **2015**, *8*, 603.
- [154] T. Kajiwara, M. Fujii, M. Tsujimoto, K. Kobayashi, M. Higuchi, K. Tanaka, S. Kitagawa, *Angew. Chem., Int. Ed.* **2016**, *55*, 2697.
- [155] L. Shi, T. Wang, H. Zhang, K. Chang, J. Ye, *Adv. Funct. Mater.* **2015**, *25*, 5360.
- [156] M. Wang, D. Wang, Z. Li, *Appl. Catal. B: Environ.* **2016**, *183*, 47.
- [157] R. Li, J. Hu, M. Deng, H. Wang, X. Wang, Y. Hu, H.-L. Jiang, J. Jiang, Q. Zhang, Y. Xie, Y. Xiong, *Adv. Mater.* **2014**, *26*, 4783.
- [158] S. Wang, W. Yao, J. Lin, Z. Ding, X. Wang, *Angew. Chem., Int. Ed.* **2014**, *53*, 1034.
- [159] D. Shi, C. He, B. Qi, C. Chen, J. Niu, C. Duan, *Chem. Sci.* **2015**, *6*, 1035.
- [160] X.-L. Yang, M.-H. Xie, C. Zou, Y. He, B. Chen, M. O'Keefe, C.-D. Wu, *J. Am. Chem. Soc.* **2012**, *134*, 10638.
- [161] J. Long, S. Wang, Z. Ding, S. Wang, Y. Zhou, L. Huang, X. Wang, *Chem. Commun.* **2012**, *48*, 11656.
- [162] D. Sun, L. Ye, Z. Li, *Appl. Catal. B* **2015**, *164*, 428.
- [163] M. A. Nasalevich, M. G. Goesten, T. J. Savenije, F. Kapteijn, J. Gascon, *Chem. Commun.* **2013**, *49*, 10575.
- [164] L. Shen, S. Liang, W. Wu, R. Liang, L. Wu, *J. Mater. Chem. A* **2013**, *1*, 11473.
- [165] S. Abedi, A. Morsali, *ACS Catal.* **2014**, *4*, 1398.
- [166] P. Wu, C. He, J. Wang, X. Peng, X. Li, Y. An, C. Duan, *J. Am. Chem. Soc.* **2012**, *134*, 14991.
- [167] A. Mahmood, W. Guo, H. Tabassum, R. Zou, *Adv. Energy Mater.* **2016**, *6*, 1600423.
- [168] M. Jahan, Q. Bao, K. P. Loh, *J. Am. Chem. Soc.* **2012**, *134*, 6707.
- [169] S. Ma, G. A. Goenaga, A. V. Call, D.-J. Liu, *Chem. Eur. J.* **2011**, *17*, 2063.
- [170] A. Aijaz, N. Fujiwara, Q. Xu, *J. Am. Chem. Soc.* **2014**, *136*, 6790.
- [171] N. L. Torad, R. R. Salunkhe, Y. Li, H. Hamoudi, M. Imura, Y. Sakka, C.-C. Hu, Y. Yamauchi, *Chem. Eur. J.* **2014**, *20*, 7895.
- [172] X. Wang, J. Zhou, H. Fu, W. Li, X. Fan, G. Xin, J. Zheng, X. Li, *J. Mater. Chem. A* **2014**, *2*, 14064.
- [173] W. Xia, J. Zhu, W. Guo, L. An, D. Xia, R. Zou, *J. Mater. Chem. A* **2014**, *2*, 11606.
- [174] S. You, X. Gong, W. Wang, D. Qi, X. Wang, X. Chen, N. Ren, *Adv. Energy Mater.* **2016**, *6*, 1501497.
- [175] A. Almasoudi, R. Mokaya, *J. Mater. Chem. A* **2014**, *2*, 10960.
- [176] N. L. Torad, M. Hu, Y. Kamachi, K. Takai, M. Imura, M. Naito, Y. Yamauchi, *Chem. Commun.* **2013**, *49*, 2521.

- [177] Y.-Z. Chen, C. Wang, Z.-Y. Wu, Y. Xiong, Q. Xu, S.-H. Yu, H.-L. Jiang, *Adv. Mater.* **2015**, *27*, 5010.
- [178] B. You, N. Jiang, M. Sheng, W. S. Drisdell, J. Yano, Y. Sun, *ACS Catal.* **2015**, *5*, 7068.
- [179] L. Shang, H. Yu, X. Huang, T. Bian, R. Shi, Y. Zhao, G. I. Waterhouse, L. Z. Wu, C. H. Tung, T. Zhang, *Adv. Mater.* **2016**, *28*, 1668.
- [180] W. Xia, R. Zou, L. An, D. Xia, S. Guo, *Energy Environ. Sci.* **2015**, *8*, 568.
- [181] Q. Li, P. Xu, W. Gao, S. Ma, G. Zhang, R. Cao, J. Cho, H.-L. Wang, G. Wu, *Adv. Mater.* **2014**, *26*, 1378.
- [182] S. Zhao, H. Yin, L. Du, L. He, K. Zhao, L. Chang, G. Yin, H. Zhao, S. Liu, Z. Tang, *ACS Nano* **2014**, *8*, 12660.
- [183] Y. Hou, T. Huang, Z. Wen, S. Mao, S. Cui, J. Chen, *Adv. Energy Mater.* **2014**, *4*, 1400337.
- [184] Q.-L. Zhu, W. Xia, L.-R. Zheng, R. Zou, Z. Liu, Q. Xu, *ACS Energy Lett.* **2017**, *2*, 504.
- [185] Q.-L. Zhu, W. Xia, T. Akita, R. Zou, Q. Xu, *Adv. Mater.* **2016**, *28*, 6391.
- [186] P. Yin, T. Yao, Y. Wu, L. Zheng, Y. Lin, W. Liu, H. Ju, J. Zhu, X. Hong, Z. Deng, G. Zhou, S. Wei, Y. Li, *Angew. Chem., Int. Ed.* **2016**, *55*, 10800.
- [187] Y. Chen, S. Ji, Y. Wang, J. Dong, W. Chen, Z. Li, R. Shen, L. Zheng, Z. Zhuang, D. Wang, Y. Li, *Angew. Chem., Int. Ed.* **2017**, *56*, 6937.
- [188] B. Nohra, H. El Moll, L. M. Rodriguez Albelo, P. Mialane, J. Marrot, C. Mellot-Draznieks, M. O'Keeffe, R. Ngo Biboum, J. Lemaire, B. Keita, *J. Am. Chem. Soc.* **2011**, *133*, 13363.
- [189] J.-S. Qin, D.-Y. Du, W. Guan, X.-J. Bo, Y.-F. Li, L.-P. Guo, Z.-M. Su, Y.-Y. Wang, Y.-Q. Lan, H.-C. Zhou, *J. Am. Chem. Soc.* **2015**, *137*, 7169.
- [190] X.-F. Lu, P.-Q. Liao, J.-W. Wang, J.-X. Wu, X.-W. Chen, C.-T. He, J.-P. Zhang, G.-R. Li, X.-M. Chen, *J. Am. Chem. Soc.* **2016**, *138*, 8336.
- [191] J.-Q. Shen, P.-Q. Liao, D.-D. Zhou, C.-T. He, J.-X. Wu, W.-X. Zhang, J.-P. Zhang, X.-M. Chen, *J. Am. Chem. Soc.* **2017**, *139*, 1778.
- [192] S. Zhao, Y. Wang, J. Dong, C.-T. He, H. Yin, P. An, K. Zhao, X. Zhang, C. Gao, L. Zhang, J. Lv, J. Wang, J. Zhang, A. M. Khattak, N. A. Khan, Z. Wei, J. Zhang, S. Liu, H. Zhao, Z. Tang, *Nat. Energy* **2016**, *1*, 16184.
- [193] H. Zhang, Z. Ma, J. Duan, H. Liu, G. Liu, T. Wang, K. Chang, M. Li, L. Shi, X. Meng, K. Wu, J. Ye, *ACS Nano* **2016**, *10*, 684.
- [194] H. Hu, B. Guan, B. Xia, X. W. Lou, *J. Am. Chem. Soc.* **2015**, *137*, 5590.
- [195] T. Y. Ma, S. Dai, M. Jaroniec, S. Z. Qiao, *J. Am. Chem. Soc.* **2014**, *136*, 13925.
- [196] G. Cai, W. Zhang, L. Jiao, S.-H. Yu, H.-L. Jiang, *Chem* **2017**, *2*, 791.
- [197] M. Xu, L. Han, Y. Han, Y. Yu, J. Zhai, S. Dong, *J. Mater. Chem. A* **2015**, *3*, 21471.
- [198] L. Jiao, Y.-X. Zhou, H.-L. Jiang, *Chem. Sci.* **2016**, *7*, 1690.
- [199] H. B. Wu, B. Y. Xia, L. Yu, X.-Y. Yu, X. W. Lou, *Nat. Commun.* **2015**, *6*, 6512.
- [200] Y.-J. Tang, M.-R. Gao, C.-H. Liu, S.-L. Li, H.-L. Jiang, Y.-Q. Lan, M. Han, S.-H. Yu, *Angew. Chem., Int. Ed.* **2015**, *54*, 12928.
- [201] R. S. Kumar, S. S. Kumar, M. A. Kulandainathan, *Electrochem. Commun.* **2012**, *25*, 70.
- [202] R. Hinogami, S. Yotsuhashi, M. Deguchi, Y. Zenitani, H. Hashiba, Y. Yamada, *ECS Electrochem. Lett.* **2012**, *1*, H17.
- [203] I. Hod, M. D. Sampson, P. Deria, C. P. Kubiak, O. K. Farha, J. T. Hupp, *ACS Catal.* **2015**, *5*, 6302.
- [204] N. Kornienko, Y. Zhao, C. S. Kley, C. Zhu, D. Kim, S. Lin, C. J. Chang, O. M. Yaghi, P. Yang, *J. Am. Chem. Soc.* **2015**, *137*, 14129.
- [205] X. Kang, Q. Zhu, X. Sun, J. Hu, J. Zhang, Z. Liu, B. Han, *Chem. Sci.* **2016**, *7*, 266.
- [206] G. Huang, Q. Yang, Q. Xu, S.-H. Yu, H.-L. Jiang, *Angew. Chem., Int. Ed.* **2016**, *55*, 7379.
- [207] X. Li, T. W. Goh, L. Li, C. Xiao, Z. Guo, X. C. Zeng, W. Huang, *ACS Catal.* **2016**, *6*, 3461.
- [208] W. Shi, L. Cao, H. Zhang, X. Zhou, B. An, Z. Lin, R. Dai, J. Li, C. Wang, W. Lin, *Angew. Chem., Int. Ed.* **2017**, *56*, 9704.
- [209] C.-D. Wu, M. Zhao, *Adv. Mater.* **2017**, *29*, 1605446.
- [210] Y.-Z. Chen, Z. U. Wang, H. Wang, J. Lu, S.-H. Yu, H.-L. Jiang, *J. Am. Chem. Soc.* **2017**, *139*, 2035.